

1 **Spatiotemporally resolved emissions and concentrations of Styrene, Benzene,**  
2 **Toluene, Ethylbenzene, and Xylenes (SBTEX) in the U.S. Gulf region**

3 Chi-Tsan Wang<sup>1</sup>, William Vizuete<sup>2</sup>, Lawrence S. Engel<sup>3</sup>, Jia Xing<sup>1</sup>, Jaime Green<sup>2</sup>, Marc Serre<sup>2</sup>,  
4 Richard Strott<sup>2</sup>, Jared Bowden<sup>4</sup>, Jung-Hun Woo<sup>5</sup>, and Bok H. Baek<sup>1\*</sup>

5 <sup>1</sup>Center for Spatial Information Science and Systems (CSISS), George Mason University, Fairfax,  
6 VA, U.S.

7 <sup>2</sup>Department of Environmental Sciences & Engineering, University of North Carolina, Chapel  
8 Hill, NC, U.S.

9 <sup>3</sup>Department of Epidemiology, University of North Carolina, Chapel Hill, NC, U.S.

10 <sup>4</sup>Departement of Applied Ecology, North Carolina State University, Raleigh, NC, U.S.

11 <sup>5</sup>Civil and Environmental Engineering, College of Engineering, Konkuk University, Seoul,  
12 Republic of Korea

13 \*Corresponding authors: Bok H. Baek (Email: bhbaek@gmail.com; Telephone: +1 919-308-6519)

14 **Abstract**

15 Styrene, benzene, toluene, ethylbenzene, and xylenes (SBTEX) are established neurotoxicants.  
16 These SBTEX are hazardous air pollutants (HAPs) and released from the petrochemical industry,  
17 combustion process, transport emission, and solvent usage sources. Although several SBTEX toxic  
18 assessment studies have been conducted, they have mainly relied on ambient measurements to  
19 estimate exposure and limiting their scope to specific locations and observational periods. To  
20 overcome these spatiotemporal limitations, an air quality modeling system over the U.S. Gulf  
21 region was created predicting the spatially and temporally enhanced SBTEX modeling  
22 concentrations from May to September 2012. Due to the incompleteness of SBTEX in the official  
23 US EPA National Emission Inventory (NEI), Hazardous Air Pollutions Imputation (HAPI)  
24 program was used to identify and estimate the missing HAPs emissions. The improved emission  
25 data was processed to generate the chemically-speciated hourly gridded emission inputs for the  
26 Comprehensive Air Quality Model with Extensions (CAMx) chemical transport model to simulate  
27 the SBTEX concentrations over the Gulf modeling region. SBTEX pollutants were modeled using

28 a "Reactive Tracer" feature in CAMx that accounts for their chemical and physical processes in  
29 the atmosphere. The data shows that the major SBTEX emissions in this region are contributed by  
30 mobile emission (45%), wildfire (30%), and industry (26%). Most SBTEX emissions are emitted  
31 during daytime hours (local time 14:00 -17:00), and the emission rate in the model domain is about  
32 20 - 40 t hr<sup>-1</sup>, which is about 4 times higher than that in the night-time (local time 24:00 – 4:00,  
33 about 4 – 10 t hr<sup>-1</sup>). High concentrations of SBTEX (above 1 ppb) occurred near the cities close to  
34 the I-10 interstate highway (Houston, Beaumont, Lake Charles, Lafayette, Baton Rouge, New  
35 Orleans, and Mobile) and other metropolitan cities (Shreveport and Dallas). High styrene  
36 concentrations were co-located with industrial sources, which contribute the most to the styrene  
37 emissions. The HAPI program successfully estimated missing emissions of styrene from the  
38 chemical industry. The change increased total styrene emissions was increased by 22% resulting  
39 in maximum ambient concentrations increasing from 0.035 ppb to 1.75 ppb across the model  
40 domain. The predicted SBTEX concentrations with imputed emissions present good agreement  
41 with observational data, with a correlation coefficient (R) of 0.75 (0.46 to 0.77 for individual  
42 SBTEX species) and normalized mean bias (NMB) of -5.6% (-24.9% to 32.1% for individual  
43 SBTEX species), suggesting their value for supporting any SBTEX-related human health studies  
44 in the Gulf region.

45 **Keywords:** BTEX, styrene, SMOKE, Reactive Tracer, Toxicants, HAP, CAMx, Exposure

46

## 47 1. Introduction

48 Styrene, benzene, toluene, ethylbenzene, and xylenes (SBTEX) are listed as Hazardous Air  
49 Pollutants (HAPs) by the U.S. Environmental Protection Agency (EPA) (Declet-Barreto et al.,  
50 2020) and can be detected in unhealthy amounts in the ambient environment. The SBTEX is  
51 primarily from industrial emission sources and can be found in the petrochemical, construction,  
52 and manufacturing industries (Polvara et al., 2021; Declet-Barreto et al., 2020) with 98% of  
53 benzene emissions attributed to coal and petroleum sources (ATSDR, 2007a, b, 2010a, b, 2017).  
54 Exposure studies of total SBTEX at industrial sources in the Middle East, Europe, and West Asia,  
55 have shown that workers experience a cumulative yearly environmental exposure of 25 - 176 ppb  
56 (Al-Harbi et al., 2020; Rajabi et al., 2020; Christensen et al., 2018; Rahimpoor et al., 2022; Niaz  
57 et al., 2015; Moshiran et al., 2021). The inhalation reference concentration for benzene shows low-  
58 dose linearity utilizing maximum likelihood estimate E-5 risk level of benzene (1 in 100,000) range  
59 is 0.4 -1.4 ppb of air concentration for leukemia (USEPA, 2000).

60 Given the importance of SBTEX from industrial sources, the heavily industrialized Gulf region of  
61 the U.S. could be a significant source of exposure for the population living there. According to the  
62 Agency for Toxic Substances and Disease Registry (ATSDR) report, the petrochemical industry  
63 in the Gulf region states contributes approximately 52% (~5.3 million tons yr<sup>-1</sup>) of benzene  
64 production capacity in the U.S. (ATSDR, 2007a) and ~75% (~6.2 million tons yr<sup>-1</sup>) of xylenes  
65 production capacity (ATSDR, 2007b). Texas and Louisiana have significant production of styrene  
66 and ethylbenzene, with an annual production of 5.5 and 7.2 million tons yr<sup>-1</sup>, respectively (SRI,  
67 2008; ATSDR, 2010a). A recent study of SBTEX exposures in the U.S. Gulf region, conducted  
68 within the Gulf Long-term Follow-up Study (GULF Study) cohort (NIEHS, 2021), observed  
69 associations of blood concentrations and annual average air concentrations of these chemicals with  
70 neurological symptoms (Werder et al., 2019; Werder et al., 2018). The average blood BTEX  
71 concentration among the 146 tobacco smoke-unexposed participants with blood measurements in  
72 this study was 255 ng L<sup>-1</sup> es (Doherty et al., 2017; Werder et al., 2018) . This value is similar to  
73 that for a representative nationwide sample assessed as part of the US National Health and  
74 Nutrition Examination Survey (NHANES) in 2005-2008 (NCHS, 2021), which measured an  
75 average of 247 ng L<sup>-1</sup>. In the GuLF Study, however, the 95<sup>th</sup> percentile of BTEX concentrations  
76 was 991 ng L<sup>-1</sup>, which is 23% higher than the 95<sup>th</sup> percentile for the NHANES nationwide sample  
77 of 803 ng L<sup>-1</sup>. The mean blood concentration of styrene for the GuLF Study sample was 52 ng L<sup>-1</sup>

78 (95<sup>th</sup> percentile: 882 ng L<sup>-1</sup>), or twice the NHANES nationwide mean of 25 ng L<sup>-1</sup> (95<sup>th</sup> percentile:  
79 55 ng L<sup>-1</sup>) (NCHS, 2021). Due to the short biological half-lives of SBTEX species, the study  
80 concluded that this high average SBTEX concentration in blood in the Gulf Region resulted from  
81 recent, presumably local emission sources.

82 Most ambient exposure studies of SBTEX have relied directly on local measurements from the  
83 field, or at existing ambient monitors. These measurements can then be used in statistical models  
84 to spatially predict exposures to SBTEX (Pankow et al., 2003; O'Leary and Lemke, 2014; Miller  
85 et al., 2018; Hsieh et al., 2020b). For example, Hsieh et al. (Hsieh et al., 2020a) developed the  
86 Multivariate Linear Regression (MLR) models to estimate SBTEX concentrations using  
87 correlations with other criteria air pollutants, including nitrogen oxides (NO<sub>x</sub>), carbon monoxide  
88 (CO), sulfur dioxide (SO<sub>2</sub>), particulate matter (PM), and meteorological conditions (temperature,  
89 wind speed). The MLR model predicted a strong correlation with NO<sub>x</sub> and CO. The limitations of  
90 the statistical model are that they require measurement data, and they assume that the  
91 measurements originate from a single source in a relatively small region. The use of a dispersion  
92 model is another way to estimate ambient SBTEX concentrations when local measurements are  
93 lacking. Chen et al., 2016 (Chen et al., 2016) applied a dispersion model to predict SBTEX and  
94 other toxicant concentrations in two industrial complexes in Kaohsiung City, Taiwan. The  
95 dispersion model performed better for stationary point sources than a statistical based model and  
96 predicted up to ~78% of the ambient observation. These dispersion models, however, only account  
97 for exposures at a smaller spatial scale (USEPA, 2022, 2023) thus cannot support regional scale  
98 (e.g., state-level) application. Furthermore, these models assumed that the exposure rate to SBTEX  
99 is linear, without considering any chemical destruction and wet/dry deposition losses in the  
100 atmosphere.

101 An accurate SBTEX assessment in the Gulf region must address the known uncertainties  
102 associated with current statistical, biometric, and dispersion model approaches. Improved accuracy  
103 in exposure estimation is dependent on the inclusion of all industrial emission sources, must  
104 capture the temporal and spatial variability known to occur in industrial emission rates, and should  
105 include the chemical and physical decay processes of the atmosphere. These issues can be  
106 addressed using a regional-scale chemical transport model (CTM), like the Comprehensive Air  
107 Quality Model with Extension (CAMx) (RAMBOLL, 2021) coupled with an emission inventory

108 that provides a comprehensive account of all SBTEX sources. Besides, the reactive tracer function,  
109 which is one of the CAMx probing tools, allows the model to explicitly simulate SBTEX  
110 concentrations. Currently, SBTEX emission data can be found in EPA's National Emission  
111 Inventory (NEI), which includes data from the Toxics Release Inventory (TRI) program database  
112 (USEPA, 2021d). Unlike for benzene sources, the TRI data for the other four species (STEX) is  
113 based on voluntary reports, and as a result, the 2011 NEI has emission rate data for these air toxics  
114 only for a limited set of emission sources (USEPA, 2021a).

115 The following work describes the development of a new STEX emission inventory for the Gulf  
116 Coast region that includes the emission sources absent from the 2011 NEI. Missing emission rate  
117 data of STEX was provided by analyzing NEI emissions of similar industrial sources that did  
118 provide emission rates and applying their rates to the missing source. Diurnal profiles for STEX  
119 were based on the hourly profiles of other pollutants with the same type of industrial source. This  
120 study then applied the Sparse Matrix Operator Kernel Emissions (SMOKE) model system (Baek  
121 and Seppanen, 2021) to generate a CAMx-ready emission inventory. Since STEX are not included  
122 as explicit species in the chemical mechanisms used by CAMx, a reactive tracer was included to  
123 account for chemical losses. This new emission inventory was then utilized in CAMx to predict  
124 STEX concentrations over the Gulf region for 5 months in 2012.

125

126 **2. Materials and Methods**

127 In this study, the 2011 version 6 NEI was applied as the base emission inventory (USEPA, 2021b).  
128 Subsequently, the SMOKE modeling system was employed to produce hourly gridded emissions  
129 of SBTEX across the Gulf modeling region for the year 2012. These SBTEX emissions were  
130 utilized in conjunction with the CTM model and a reactive tracer function to generate the SBTEX  
131 concentration map. In the end, the USEPA Ambient Monitoring Technology Information Center  
132 (AMTIC) data were employed to evaluate the model performance in simulating SBTEX  
133 concentrations.

134 **2.1 Emission Data Preparation**

135 **2.1.1 The HAPs Emissions in NEI**

136 The NEI is a national database providing comprehensive annual air emission estimates for both criteria  
137 air pollutants (CAPs) (e.g., CO, NO<sub>x</sub>, SO<sub>2</sub>, NH<sub>3</sub>, VOC, and PM<sub>2.5</sub>), and HAPs (e.g., benzene,  
138 acetaldehyde, formaldehyde, xylenes, styrene, and more) from all types of emissions sources (e.g.,  
139 point, nonpoint, and mobile). While CAPs emissions are reported by the state agencies is mandatory, the  
140 report of HAPs is usually voluntary. Consequently, only a limited set of HAPs have been reported to  
141 the USEPA, and their spatial coverage can vary significantly by source type (e.g., industrial,  
142 vehicles) and region (e.g., county and state) (Strum et al., 2017).

143 The VOC emission species generated by SMOKE from NEI have three types which are “model  
144 surrogate”, “model explicit”, and “HAPs explicit” species. The “model surrogate species”, such as  
145 XYL (xylene and other poly-alkyl aromatics), TOL (toluene and other mono-alkyl aromatics), and  
146 PAR (paraffin carbon bond), are calculated by speciation profiles in emission model platform and  
147 used to predict ozone and secondary organic aerosol (SOA) in the CTM but not for individual  
148 HAPs emission and simulation. Only five HAP emissions in NEI are “model explicit” specie:  
149 Naphthalene (NAPH), benzene (BENZ), Acetaldehyde (ALD2), Formaldehyde (FORM), and  
150 Methanol (MEOH), known as "NBAFM" to represent their individual emission (Strum et al., 2017),  
151 and are directly processed in CTM model, too. The “HAPs explicit” species emission in NEI  
152 includes hundreds of toxicants (such as styrene, xylenes, Mercury, and Acrolein). Those “HAPs

153 explicit” species cannot be directly used in the current CTM model because their explicit chemical  
154 mechanisms are not developed in the current CTM chemical mechanism.

155 The “model explicit” species, benzene (B), and other “HAPs explicit” species, including styrene,  
156 toluene, ethylbenzene, and xylenes (STEX) are targeted for this SBTEX human exposure study.  
157 The SMOKE model system (Baek and Seppanen, 2021) assigned the annual or monthly SBTEX  
158 emission inventory in NEI to hourly emission patterns by the temporal profiles based on emission  
159 processes and locations by Source Category Code (SCC) and Federal Information Processing  
160 Standards (FIPS) county codes. These processes are coupled with the CAPs when generating the  
161 CTM-ready emission data.

### 162 **2.1.2 Imputation of NEI with STEX**

163 Considering that Benzene emission reporting is mandatory in the NEI and thus can be assumed to  
164 have no significant missing sources, we only focused on the investigation of missing sources for  
165 the STEX which is voluntary reporting. This study utilized the 2011 NEI summary reports from  
166 the SMOKE modeling System (Baek and Seppanen, 2021) to identify those missing STEX  
167 emission sources. The SMOKE reports provided the annual or monthly total of VOC and  
168 individual HAPs emissions sorted by SCC and FIPS county codes. This study developed an R-  
169 project (The R Foundation, 2021) program called "*Hazardous Air Pollutants Imputation*" (HAPI)  
170 that can first read the reports from SMOKE and identify the list of inventory sources reported  
171 without STEX toxics. Then it generates the imputation data for those missing STEX inventory  
172 sources based on the proxy of STEX and VOC for those emission sources that share the same SCC  
173 near the region (county or state).

174 Theoretically, the SCC is the reference code defining the emission process type. The same SCC  
175 means they share similar emission factors with the same emission process (USEPA, 2016). The  
176 profiles of HAPs for the VOC can be shared with those same SCC emission sources within the  
177 surrounding regions (counties or states)(Strum et al., 2017). When there are the same SCC  
178 emission sources with zero HAPs in other counties, this study performed the imputation of those  
179 missing HAPs emissions based on the HAPs profiles from the matched emission source. For  
180 example, the HAPs profile of styrene and toluene to the VOC emission is defined as the ratio of

181 styrene and toluene emissions over the VOC emission ( $P_{toluene,s}$ ) in counties where there are  
 182 styrene, toluene, and VOC emissions for that SCC ( $s$ ). Then, this study will assume that those  
 183 HAPs are missing when the summation of HAPs emissions are zero ( $\sum_i E_{i,s,f} = 0$ :  $i$  is pollutants,  
 184  $s$  is SCC code,  $f$  is FIPS county code) but VOC emission is available. Then this will apply the  
 185 HAPs profile for the same SCC to the existing VOC and estimate missing styrene and toluene  
 186 emissions. Therefore, this process can impute the missing HAP emissions based on the SCC-  
 187 matched HAPs fractions from the surrounding counties or the same state.

188 The HAPI was developed based on this imputation concept. This study first separated the county  
 189 and SCC level inventory data into two groups in the HAPI program: "with HAPs" and "without  
 190 HAPs." For the "with HAPs" group, summations of HAPs emissions in counties and SCCs are not  
 191 zero. In contrast, for the "without HAPs" group, summations of HAPs emissions in counties and  
 192 SCC are zero.

193 In the "with HAPs" group ( $\sum_i E_{i,s,f} > 0$ ) in Eq. (1),  $i$  is the individual HAP, such as styrene,  
 194 benzene, toluene, ethylbenzene, xylenes, Acrolein, and 1,3-Butadiene;  $s$  is the SCC, and  $f$  is the  
 195 county FIPS code for county.  $E_{i,s,f}$  is the annual emission of pollutant  $i$  for SCC in the county.  $E_{voc,s,f}$   
 196 is the CAP VOC emission for the SCC in the county. The HAPs profile ( $P_{i,s}$ ) is a fraction of HAP-  
 197 specific emission ( $E_{i,s,f}$ ) over the summation of matched SCC and county-specific VOC emission  
 198 ( $E_{voc,s,f}$ ) from the "with HAPs" group.

199 This study assumed that if there is an SCC-matched "with HAPs" group HAPs profile in the  
 200 inventory, they are not considered as missing HAPs emission sources. Only the emission sources  
 201 for which the sum of all HAPs is zero ( $\sum_i E_{i,s,f} = 0$ ) are considered as the "without HAPs" group."  
 202 In Eq.(2),  $P_{i,s}$  is used to estimate those missing HAPs for the "without HAPs" inventory source  
 203 group. The  $E_{voc,s,f}$  is the CAP VOC emission in the "without HAPs" group.

204 When  $\sum_i E_{i,s,f} > 0$ , calculate individual HAPs to total VOC ratio ( $P_{i,s}$ ):

$$P_{i,s} = \frac{\sum_f E_{i,s,f}}{\sum_f E_{voc,s,f}} \quad \text{Eq. (1)}$$

206 When  $\sum_i E_{i,s,f} = 0$ , the HAPs emission are missing, this study applied  $P_{i,s}$  and VOC emission to  
 207 estimate the missing HAPs emission:



208 
$$Em_{i,s,f} = P_{i,s} \times E_{voc,s,f} \quad \text{Eq. (2)}$$

209 The HAPI program then outputs the total HAPs emissions ( $Em_{i,s,f}$ ) for the SMOKE modeling  
210 system to integrate with the CAP VOC inventory described in Section 2.1.2. Finally, the HAPI  
211 program performs the quality assurance step again to confirm that there are no missing HAPs after  
212 imputation and that the summation of HAPs emissions is not greater than the CAP VOC emission.

## 213 **2.2 Model Configuration**

### 214 **2.2.1 Air Quality Modeling**

215 The Comprehensive Air Quality Model with Extensions version 7.0, CAMx7.0 (RAMBOLL  
216 2020) was implemented in this study to simulate the SBTEX concentrations in the atmosphere.  
217 The model simulation period is from April 20<sup>th</sup> to September 30<sup>th</sup>, 2012 (April 20<sup>th</sup> to April 30<sup>th</sup>  
218 are spin-up dates). The evaluated meteorological data from WRF version 3.8 over the U.S.  
219 continental region are provided by the USEPA Support Center for Regulatory Atmospheric  
220 Modeling (SCRAM) (USEPA, 2022). The WRF output data were transformed into SMOKE-ready  
221 gridded hourly meteorology through the Meteorology Chemistry Interface Processor (MCIP). The  
222 emissions sectors modulated by meteorology, such as onroad (Choi et al., 2014; Lindhjem et al.,  
223 2004) and biogenic, were estimated with the MCIP gridded hourly meteorology. The USEPA's  
224 2012 daily total wildfire emissions (ptfire) estimated by SMARTFIRE2 (USEPA, 2015) were also  
225 incorporated (USEPA, 2021b). Additionally, the WRF meteorological data were converted to  
226 CAMx-ready meteorological data by using WRFCAMx (RAMBOLL, 2020b) for the CAMx  
227 model input. The photodissociation coefficients are calculated by the Tropospheric Ultraviolet-  
228 Visible (TUV) Radiation Model (Madronich, 1987) with Ozone Monitoring Instrument (OMI)  
229 daily data (NASA, 2021). The USEPA daily hemisphere CMAQ model results are used to  
230 calculate the boundary condition and initial condition (Hogrefe et al., 2021). The chemical  
231 mechanism is Carbon Bond 06 revision 4 (CB6r4) (Ramboll, 2020a). Figure 1 in manuscript shows  
232 that the model domain is 12 km × 12 km (blue rectangle). We also 4 km × 4 km (red rectangle)  
233 nesting simulation to enhance the model spatial resolution through the flexi-nesting method. The  
234 point source emissions are processed independently with their stack locations in the model domain

235 and considering the plume-raising effect by stack parameters. As a result, the model spatial  
236 allocations can be enhanced through the flexi-nesting method.

237 The modeling ozone evaluation results over the simulation period are shown in Table S2. The  
238 evaluation indicators followed the USEPA's model evaluation guidance (USEPA, 2006). The  
239 modeling ozone is fairly performed well over the Gulf region states (Correlation Coefficient ( $R$ )  $\geq$   
240 0.55). The simulated ozone in Texas and Louisiana are close to the observation data in USEPA  
241 AQS stations (Texas:  $R = 0.79$ ,  $NMB = 1\%$ ; Louisiana:  $R = 0.77$ ,  $NMB = 11\%$ ). Additionally,  
242 because our model shares the same simulation period as the Texas Commission on Environmental  
243 Quality (TCEQ) 2012 Ozone SIP modeling application (TCEQ, 2016), we verified our modeling  
244 results with TCEQ's simulated OH radical-related model species, including  $O_3$ ,  $NO_2$ , and  
245 formaldehyde over the Dallas and Houston region (Fig. S2). The detailed comparisons are shown  
246 in the supplementary documents and indicate that both modeling applications share a similar, good  
247 modeling performance.

### 248 2.2.2 Reactive Tracer

249 The overall research method scheme flowchart is shown in Fig. 2. After developing the CTM-  
250 ready emissions and CAMx model for oxidants species (OH,  $O_3$  and  $NO_3$ ), the "Reactive Tracer"  
251 (RTRAC) was used to simulate the ambient SBTEX concentration over the Gulf region. The  
252 "Reactive Tracer" is a probing tool in the CAMx modeling system to simulate explicit SBTEX  
253 concentrations. Along with the physical transport processes (diffusion and advection) and decay  
254 processes like wet and dry deposition same as the core model, there is the second-order chemical  
255 reduction rate  $r$  that is calculated using the oxidants (Ozone, OH,  $NO_3$ ) concentrations [ $Ox$ ], the  
256 SBTEX concentrations [ $Tr$ ], and the rate constants of reactions  $k_{Tr+Ox}$  (Eq.3). In Eq.4,  $k$  is the rate  
257 constant calculated by  $A$ ,  $B$ , temperature ( $T$ ), and activation energy ( $E_a$ ). The Master Chemical  
258 Mechanism for aromatic schemes (Bloss et al., 2005) is considered for the parameters of each  
259 specific reaction in the RTRAC process.

260 This study considered the initial reactions of SBTEX in the MCM mechanism version 3.3.1 (Jenkin  
261 et al., 2015). For other parameters, the National Institute of Standards and Technology (NIST)  
262 Chemistry Webbook (P.J. Linstrom and W.G. Mallard, 2018), and CAMx user guide (RAMBOLL,

263 2020b) are considered for determining the Henry's Law constant, dependence temperature, and  
264 molecular weight. All parameters used in our RTRAC modeling are presented in Tables S3 and  
265 S4.

$$266 \quad r = k_{Tr+Ox} [Tr][Ox] \quad \text{Eq. (3)}$$

$$267 \quad k = A\left(\frac{T}{300}\right)^B \exp\left(\frac{-E_a}{T}\right) \quad \text{Eq. (4)}$$

268 The simulated SBTEX concentration will be evaluated by comparing against with observational  
269 data which will be described in the following.

### 270 **Ambient SBTEX Measurements**

271 The CAMx modeling evaluation was completed with the USEPA Air Quality Station (AQS) ozone  
272 observational data and the Texas Commission on Environmental Quality (TCEQ) State  
273 Implementation Plan (SIP) ozone modeling output data (TCEQ, 2015). The measured ambient  
274 SBTEX concentrations are from the USEPA Ambient Monitoring Technology Information Center  
275 (AMTIC), which is an observational network that routinely detects more than 100 air toxics in the  
276 U.S. (USEPA, 2021c). It includes the federal and state monitoring stations. The 5 months (May to  
277 September 2012) individual SBTEX concentrations from the AMTIC were utilized to evaluate the  
278 RTRAC modeling results from CAMx.

279 A total of 46 monitoring sites measure SBTEX concentrations within our 4 km × 4 km model  
280 domain, and most of them are located within Texas (42 sites), except for four sites in Louisiana.  
281 The air sampling duration can be 1-hour, 3-hour, or 24-hour. There are six monitoring sites with  
282 1-hour measurement data in Texas, three sites with 3-hour data in Louisiana, and the rest with 24-  
283 hour data. The AMTIC sites are indicated in Fig. 1 with red stars. The USEPA conducted QA/QC  
284 for the AMTIC data, which contain values that are exceptionally high due to unpredictable  
285 industrial VOC release events (Couzo et al., 2012). These events are beyond the regulatory  
286 emission counting; thus, the model cannot capture those unpredictable events, particularly in  
287 petrochemical, oil, and gas industrial areas. Therefore, this study removed outliers (those beyond  
288 twice the interquartile range (2×IQR) above Q3) for better evaluating the model performance in  
289 simulating the SBTEX concentration in general.

290 The CAMx RTRAC modeling results are spatially and temporally resolved gridded hourly  
291 concentrations, while the AMTIC observational data are from specific locations with time gaps.  
292 Daily average and diurnal pattern analyses evaluate the predicted SBTEX concentrations. For each  
293 AMTIC site, this study used the average concentration of the center grid cell and eight other  
294 "surrounding" grid cells (i.e., the average of 3×3 grid cells) to compare with the observational data  
295 (USEPA, 2006).

296

## 297 3. Results

### 298 3.1 SBTEX Emissions

299 The 2012 annual total SBTEX emissions in the model domain are shown in Table 1. The emission  
300 sectors include: agriculture fire (afgfire), commercial marine vessel (cmv), non-point source  
301 (nonpt), non-road vehicle (nonroad), on-road vehicle (onroad), fire emission (ptfire), rail road  
302 (rail), residential wood combustion (rwc), non-point oil gas industry (np\_oilgas), electricity power  
303 plants unit (ptegu), point source emission other than electricity generation unit (ptnonipm), and  
304 point source of oil and gas industry (pt\_oilgas). The largest contributor of SBTEX emissions in  
305 the 12km×12km model domain is indicated to be from the “onroad” sector, with 89,204 t yr<sup>-1</sup>,  
306 representing about 36% of the total SBTEX emissions. The “onroad” sector contributes the most  
307 of total xylenes (46%), toluene (48%), and ethylbenzene (60%) emissions, while much less to  
308 benzene (13%) and styrene (6.8%). The second largest contributor of SBTEX emissions is the  
309 “wildfire” sector (61,316 t yr<sup>-1</sup>), contributing about 25% of total SBTEX. The wildfire contributes  
310 the most of total benzene (57%), 12% of total toluene and 7% of total xylenes, but no ethylbenzene  
311 and styrene due to missing explicit profiles in the 2012 wildfire emission inventory. The “nonroad”  
312 sector ranked third (35,375 t yr<sup>-1</sup>), contributing about 14% of total SBTEX over our modeling  
313 region. The nonroad contributes largely to xylenes (15%), toluene (21%), and ethylbenzene (21%).  
314 Compared to other sectors, emissions from non-electricity generation unit industrial point sources  
315 (ptnonipm) contain a larger portion of styrene, 2,911 t yr<sup>-1</sup>, which is 69% of total styrene emission.  
316 Our study successfully identified missing styrene emissions from the chemical industry process  
317 (see table S7), leading to a 34% increase in total styrene emissions.

318 The individual and total SBTEX annual emission spatial plots in 12km×12km model domain are  
319 presented in Fig.3. The grid cell with the highest SBTEX emissions is found in Houston city near  
320 the ship channel (1059 t yr<sup>-1</sup>), which is about 35 times higher than average emission (28 t yr<sup>-1</sup>)  
321 across the domain, followed by one in San Antonio in Texas (1022 t yr<sup>-1</sup>) and one near Sabine  
322 Lake in Louisiana (1022 t yr<sup>-1</sup>). In Fig.3 (b), the missing sources of SBTEX emissions in the NEI  
323 are mostly located in Texas and Louisiana, particularly for the grid cells in Lake Charles (increased  
324 by 373 t yr<sup>-1</sup>, +282%), Baton Rouge (167 t yr<sup>-1</sup>, +31% ) in Louisiana; Belton (61 t yr<sup>-1</sup>, +21%),  
325 Fort Worth (50 t yr<sup>-1</sup>, +85%), Dallas (44 t yr<sup>-1</sup>, +52%) in Texas, and some rural areas in Texas.

326 These missing sources of SBTEX are mostly from the np\_oilgas and ptnonipm emission sectors  
327 (detailed in Supplementary document 3.1 and 3.2). Although the total SBTEX emission increased  
328 by only 2% based on the domain average (Table 1), the localized impacts for certain areas can be  
329 up to 60% of the total SBTEX emissions.

330 The SBTEX emissions exhibit strong diurnal variations across a day, as presented in Fig. 4a. The  
331 daytime hourly emission (up to 77 t hr<sup>-1</sup>) is about 4.3 times higher than the night-time emission  
332 rate, mainly due to the larger emissions from on-road and off-road mobile sources (half of total  
333 emissions) during the daytime. The diurnal variations in the chemical composition of total SBTEX  
334 also suggested the increased percentage of toluene and xylenes (indicating the transport sources)  
335 during the morning (L.T. 6:00 – 10:00) and evening (L.T. 19:00) rush hour. The inclusion of the  
336 missing sources will slightly reduce the emission variation across a day, as most of the missing  
337 sources come from industrial manufacturing and oil processes (detailed in SI) whose diurnal  
338 profiles are much flatter (about only 20% increase during the daytime) compared to the total  
339 emission (see Fig. 4b), with much smaller differences between day (0.86 t hr<sup>-1</sup>) and night (0.69 t  
340 hr<sup>-1</sup>). The chemical composition of missing emission sources were relatively constant throughout  
341 the day with about 50% comprised of xylenes, 30% toluene, and styrene was 10-15%. The relative  
342 amount of missing styrene was higher than that found in total emissions.

### 343 **3.2 Model performance**

344 CAMx simulations predicting SBTEX concentrations were completed using two sets of emissions:  
345 the National Emission Inventory (Base), and the emission scenario adjusted in this study (Adj).  
346 The differences between the two scenarios can be regarded as the impacts of the missing emission  
347 sources in the original NEI, suggesting the importance of the completeness of emissions.

348 The simulated concentrations were compared with the observations to evaluate the accuracy of  
349 SBTEX emission and concentration estimated in this study. The normalized mean bias (NMB, %)  
350 and correlation coefficient (R) of both Base and Adj cases were compared in Table 2. Overall, the  
351 CAMx model can capture the pollution level and spatiotemporal variation of all SBTEX species.  
352 More specifically, the model reproduced the daily variation of SBTEX concentrations, with R of  
353 0.65 (0.54-0.65 for individual SBTEX) for all daily observational records (N=2,717), as well as

354 their spatial distribution across observational sites (N=46, averages of the whole simulation  
355 period), with R of 0.75 (0.46 to 0.77 for individual SBTEX species), and NMB of -5.6% (-24.9%  
356 to 32.1% for individual SBTEX species).

357 The inclusion of emissions can slightly improve the overall model performance with decreased  
358 NMBs for toluene (+3.5%), xylenes (+5.7%), ethylbenzene (+3.8%), and total SBTEX (+3.2%).  
359 The NMB for styrene is increased from 17.4% to 32.1%, while R is increased by 0.01, suggesting  
360 better correlations with the new-estimated emission data, while uncertainties associated with  
361 emission factors or other parameters lead to the overestimation of SBTEX. Fig. 5 shows the spatial  
362 distribution of average concentration simulated in the Adj case, overlapping the average  
363 observational data for total SBTEX (5a) and individual species (5b to 5f). The observational data  
364 (diamond shapes) shows a high concentration in industrial or city sites, and a lower concentration  
365 at rural sites. The model results showed a continual concentration gradient pattern from cities to a  
366 rural area with 4 km × 4 km resolution and the results are close to the observational data in  
367 Houston, Dallas, Beaumont, and Baton Rouge.

368 We further classified the observation sites into four groups, including “Airport”, “Industry”,  
369 “Rural”, and “Urban” based on their geographical locations (Table S8). For total SBTEX (Fig. 6a),  
370 the correlation coefficient (R) is 0.75 (R-square is 0.56) across all locations, and the black solid  
371 line is the regression line for all sites (N=46). The red dots indicated that the industrial sites have  
372 a higher concentration in both model and observational results, and the cities (blue diamonds)  
373 showed that their concentrations are slightly overestimated and lower than industrial sites. The  
374 Airport (black squares) and Rural (green triangles) have lower SBTEX concentrations than City  
375 and Industry, and Rural is the lowest group. Fig. 6b to 6f are similar plots for explicit benzene,  
376 toluene, xylenes, ethylbenzene, and styrene. The R ranges from 0.46 to 0.77. The benzene (R is  
377 0.68), toluene (R is 0.46), and styrene (R is 0.64) are overestimated, but xylenes (R is 0.77),  
378 ethylbenzene (R is 0.77) are close to observational data. Although toluene has the lowest R (0.46),  
379 which is caused by two industry sites that largely underestimate in Houston (Site ID: 482011015)  
380 and Nederland (Site ID: 482450014), in case we remove those two industrial sites data, the R for  
381 toluene in Fig. 6c will become 0.7 (Fig. S7). This phenomenon is probably caused by the missing  
382 toluene industrial sources near those two sites. The inclusion of missing emission sources  
383 definitively improved the model performance (Table 2), especially in Rural (+5.4%) and Airport

384 groups (+6.8%) which suffered the most due to the missing industrial sources. The NMBs for  
385 xylenes are also reduced across all emission groups (Industry: +3%, Urban: +12%, Airport: +20%,  
386 and Rural: +13%).

387 Because only few sites have hourly data, this study compared the diurnal variation of SBTEX  
388 concentrations for Houston industry area (using data from only three monitoring sites) in Fig. S8.  
389 The hourly data shows that benzene, ethylbenzene, and styrene are overestimated (NMB for  
390 benzene is 69%, ethylbenzene is 36%, and styrene is 27%) during nighttime hours (LT 21:00 to  
391 6:00). Toluene is underestimated at nighttime (NMB is -45%), whereas xylenes closely aligns with  
392 the observed data (-16%) range. On the other hand, all species experience underestimation during  
393 daytime hours (NMB for benzene is -25%, Toluene is -65%, Xylenes is -51%, ethylbenzene is -  
394 46%, and Styrene is -82%) (from LT 10:00 to 17:00). Such results indicate that the hourly emission  
395 rate may overestimate during nighttime but underestimate during the daytime in Houston industry  
396 area.

### 397 **3.3 SBTEX Concentrations Patterns**

#### 398 **3.3.1 Spatial Distribution**

399 Figure 7a presents the spatial distribution of SBTEX concentration during the model period (May  
400 1st to Sep 30th) in the Adj scenario. The highest SBTEX concentration (3.07 ppb) occurs near  
401 Lake Charles, followed by Baton Rouge (2.06 ppb), Houston ship channel (2.04 ppb), Shreveport  
402 (1.69 ppb), Beaumont (1.59 ppb). The spatial distribution patterns of individual SBTEX  
403 compounds exhibit similarities due to shared emission sources, except for styrene. Styrene  
404 primarily originates from ptnonipm, while other species predominantly arise from vehicle  
405 emissions and wildfires. benzene (max: 1.06 ppb), toluene (max: 1.01 ppb), and ethylbenzene  
406 (max: 0.16 ppb) reach their highest concentrations in Houston, reflecting their significant  
407 emissions. Further, xylenes (0.78 ppb) originate from sources in Shreveport. Remarkably elevated  
408 concentrations of styrene (reaching 1.97 ppb) are conspicuously identified proximal to Lake  
409 Charles, a locale characterized by an abundant emission of styrene from non-Electricity Generating  
410 Unit point sources, which have been absent in the original NEI records.



411 This study further investigated the influence of missing emission sources in the original NEI on  
412 the SBTEX concentrations by taking the differences between Adj and Base scenarios. The majority  
413 of missing emissions are associated with the np\_oilgas and ptnonipm sectors, with increased  
414 contributions geographically concentrated in Texas and Louisiana (Fig. 7b). In particular, the  
415 largest impact on SBTEX concentration is shown near Lake Charles by up to 1.82 ppb (+68%),  
416 which is mostly related to the increase of styrene concentration (by 1.75 ppb, +5315%). This  
417 increase is due to the NEI missing one large point source (364.12 t yr<sup>-1</sup>) in the ptnonipm sector  
418 near Lake Charles. The inclusion of missing emission sources also led to the increase of styrene  
419 concentrations in other cities, such as Baton Rouge (0.07 ppb, +389%), LA, and Houston, TX  
420 (0.03 ppb, +62%). Baton Rouge, LA also suffers the largest increase of toluene concentrations by  
421 0.44 ppb (+92%) due to the inclusion of missing emissions, followed by Beaumont (0.07 ppb,  
422 +50%), and Carthage (0.048 ppb, +66%) in TX. Fort Worth, TX exhibits the most increase of  
423 xylenes concentrations by 0.07 ppb (+95%), followed by Center (0.06 ppb, +273%), Teague (0.06  
424 ppb, +340%), and Beaumont (0.036 ppb, +70%) in TX. The largest increase of ethylbenzene  
425 concentration occurred at Longview (0.01 ppb, +85%), followed by Beaumont (0.009 ppb, +40%)  
426 and Houston (0.006 ppb, +9%) in TX.

### 427 3.3.2 The Diurnal Variation

428 In general, the diurnal variations of SBTEX concentrations are primarily influenced by various  
429 factors (such as ventilation, emissions, diffusion, deposition, and chemical reactions). These  
430 variations typically manifest with lower concentrations during the daytime compared to nighttime  
431 due to increased ventilation, diffusion, and chemical loss, even though emissions are about 4 times  
432 higher during the daytime, as presented earlier (Fig. 4). Diurnal meteorological and emission  
433 patterns suggest more sensitivity of the concentrations to the emissions during nighttime than  
434 daytime, implying that implementing emission controls to reduce the concentrations at night would  
435 be most effective. The variation of emission sources might also modulate the diurnal pattern in  
436 concentrations. To demonstrate that, here we selected two industrial locations and one city location  
437 with high SBTEX concentrations to compare the diurnal variation of concentrations.

438 The first one is Channelview city (Latitude: 29.8, Longitude: -95.12), located at the Houston ship  
439 channel industrial area on the eastern side of downtown Houston. Driven by both emission

440 temporal profiles and meteorological conditions, the peak SBTEX concentration (about 12 ppb) in  
441 Channelview city occurs at LT 23:00 to 1:00, contributed mostly by benzene (56%) which  
442 indicates the industrial sources, with a small amount of toluene (19%), xylenes (13%), styrene  
443 (4.8%), ethylbenzene (7%) (Fig. 8a). The second case, Bayland Park (Latitude: 29.69, Longitude:  
444 -95.49), located nearby at the western side of Houston, presents the same level of peak SBTEX  
445 concentration (about 12 ppb) (Fig.9a) as Channelview city. In contrast to Channelview, the peak  
446 concentration of Bayland Park occurs at traffic rush hour (LT 7:00 to 8:00), contributed mostly by  
447 toluene (53%) and xylenes (23%) (indicating the mobile vehicle sources) rather than benzene  
448 (18%). Meanwhile, the adjusted industry emission sources, as presented in table S5, play a  
449 significant role in driving the peak concentration (0.4 ppb) in Channelview city (Fig. 8b), yet  
450 exhibit a reduced impact on Bayland Park (Fig. 9b), where is far from the industry area.

451 A similar pattern is also shown in Baton Rouge, Louisiana (Latitude: 30.46, Longitude: -91.17),  
452 located near downtown Baton Rouge (affected by onroad sources), and also close to the industry  
453 area (~ 1 mile from the north). Like Houston industry area, the daytime SBTEX concentration is  
454 much lower (<3 ppb) than night-time, and the peak SBTEX concentration (about 9.4 ppb) occurs  
455 at LT 22:00 (Fig. 10). Because Baton Rouge is impacted by both traffic and industrial sources,  
456 emissions differ from Houston in that both benzene (35% – 40%) and toluene (35% - 40%) become  
457 the major portion of SBTEX (Fig. 10a). The missing emission sources (Fig. 10b) will further  
458 enhance the peak concentration by 2 ppb at LT 5:00 - 8:00, with the largest chemical contribution  
459 from toluene (about 70 - 85%), followed by styrene (about 7 - 20%) associated with the industrial  
460 sources.

#### 461 **4. Conclusion and Discussion**

462 To address the urgent need for health assessment of SBTEX exposures in the Gulf region, this  
463 study developed high spatiotemporally resolved emissions and concentrations of individual  
464 SBTEX. The HAPI program was developed and implemented to identify and gap-fill the missing  
465 SBTEX inventory for the SMOKE emissions modeling system. Then the state-of-the-science  
466 chemical transport modeling system, CAMx, was applied to generate the high temporal and spatial  
467 resolution predictions of explicit SBTEX concentrations based on the improved SBTEX emission  
468 inventory and a "Reactive Tracer" (RTRAC) feature. The modeled average SBTEX concentrations

469 exhibit good agreement with observational data (R is 0.75 and NMB is improved in Adj case to -  
470 5.6% for total SBTEX), suggesting that the emissions and concentrations estimates developed in  
471 this study can be used to support well the SBTEX-related human health studies in the Gulf region.

472 This study found that the “onroad” sector contributes the most to total xylenes (46%), toluene  
473 (48%), and ethylbenzene (60%) emissions, while the styrene emissions are mostly contributed by  
474 non-EGU point sources (ptnonipm, 69%) but were substantially underestimated in the original  
475 NEI data, resulting in 34% underestimation of total styrene emissions. The highest SBTEX  
476 concentration (3.07 ppb) occurs near Lake Charles, followed by Baton Rouge (2.06 ppb), Houston  
477 ship channel (2.04 ppb), Shreveport (1.69 ppb), Beaumont (1.59 ppb), corresponding to a large  
478 amount of SBTEX emissions in these cities.

479 The 5-month average SBTEX modeled concentrations are close to the average measurement data  
480 (R of total SBTEX is 0.74, benzene is 0.68, toluene is 0.45, xylenes is 0.77, ethylbenzene is 0.77,  
481 and styrene is 0.64). These spatiotemporally fine modeled air SBTEX concentrations can be used  
482 for conducting epidemiologic analyses or in risk assessment. The diurnal variation of SBTEX  
483 concentrations that is opposite to its emissions pattern indicates that the concentration is more  
484 sensitive to emission at night than daytime. The high SBTEX concentration during nighttime  
485 affects individuals who engage in more nighttime activities or reside in houses lacking isolation  
486 of outdoor air. Therefore, the HAPs emission control policy should also focus on night-time  
487 emissions. Further, the hourly SBTEX data can be used in epidemiologic analyses to investigate  
488 effects of acute exposures and short-term changes in those exposures.

489 This study acknowledges the considerable uncertainties in this approach, including the accuracy  
490 of emission data, the meteorological condition data, and oxidants concentrations (OH radical, O<sub>3</sub>,  
491 and NO<sub>3</sub>) simulation in the CB6 mechanism. There are limited observational data to verify the  
492 model performance. This study is mainly based on the bottom-up NEI dataset, thus the  
493 uncertainties in the original NEI emissions and SMOKE process influenced on this study. For  
494 example, despite our implementation of imputation for the HAPs annual data, the emission activity  
495 within hourly, daily, and monthly temporal profiles as well as parameters (e.g., emission rates, and  
496 compositions) also remains unchanged. The emergency emissions from unreported flaring (such  
497 as final treatment equipment) or leakage events that have not been considered in the original NEI,

498 also not included in this study. Further, the concentrations of oxidants are simulated in the CAMx  
499 model with the CB6r4 mechanism; this mechanism is designed to simulate ozone and PM.  
500 Therefore, the model species OH radical, NO<sub>3</sub>, and O<sub>3</sub> may differ from the actual concentrations.  
501 These oxidant concentrations affect the chemical decay rate, especially in big metropolitan cities  
502 with higher NO<sub>x</sub> emissions. Nevertheless, the high spatiotemporally resolved emissions and  
503 concentrations of individual SBTEX developed in this study, with acceptable performance, can be  
504 a good reference dataset to support SBTEX-related human health studies in the Gulf  
505 region. Besides, this approach can be extended to other chemical compounds to estimate their  
506 concentrations. The USEPA provides emission data for approximately one hundred HAPs in the  
507 NEI for certain emission sources. Those emission data can also be processed to derive HAPs  
508 concentrations. The dataset provided in this study will facilitate epidemiologic studies of SBTEX  
509 exposures in relation to a range of health outcomes in the Gulf region and can be extended to  
510 provide similar health research opportunities elsewhere.

511

512 **Code availability:**

- 513 1. The source code of the CAMx7.00 model and model preprocess tools (O3map, tuv4.8,  
514 wrfcamx, camq2camx) can be downloaded on the Environ website:  
515 <http://www.camx.com> (RAMBOLL, 2021)  
516 2. Python 2.7 is used to treat the model output and can be downloaded on anaconda python  
517 website: <https://www.anaconda.com/distribution/> (Anaconda, 2020)  
518 3. R project for statistical computing can be downloaded at <https://www.r-project.org> (The  
519 R Foundation, 2021)  
520 4. HAPI program code can be downloaded on GitHub: <https://github.com/tatawang/HAPI>  
521 (Wang and Baek, 2023)

522

523 **Data availability:**

- 524 1. The result of this study, including SBTEX emission, concentration data and evaluation  
525 code in this study can be downloaded at: <https://zenodo.org/record/8303346>, DOI:  
526 10.5281/zenodo.8303346 (Wang et al., 2023)  
527 2. Beside the 2019 May to September, we also provided the whole 2012 SBTEX hourly  
528 concentration data of Adj case in NetCDF format and “comma-separated values (csv)”.  
529 3. The 2011 NEI emission model platform (EMP) and SMOKE model system can be  
530 downloaded on the EPA ftp website: [https://www.epa.gov/air-emissions-modeling/2011-](https://www.epa.gov/air-emissions-modeling/2011-version-6-air-emissions-modeling-platforms)  
531 [version-6-air-emissions-modeling-platforms](https://www.epa.gov/air-emissions-modeling/2011-version-6-air-emissions-modeling-platforms) (USEPA, 2021b)  
532 4. The meteorological data can be found on CMAS Data Warehouse website:  
533 <https://dataverse.unc.edu/dataverse/emascenter> (UNC-IE, 2021)  
534 5. The AMTIC data can be found at: [https://www.epa.gov/amtic/amtic-ambient-monitoring-](https://www.epa.gov/amtic/amtic-ambient-monitoring-archive-haps)  
535 [archive-haps](https://www.epa.gov/amtic/amtic-ambient-monitoring-archive-haps) (USEPA, 2021c)

536 **Author contribution**

537 CTW and BHB are the lead researchers in this study and are responsible for research design,  
538 producing data, experiments, results analysis, and manuscript writing. WV and JX are co-head  
539 researchers and guided the research design, assessed model results, and contributed to writing

540 the manuscript. JG, MS, RS, LE, JB, and JHW helped to collect and verify data and write the  
541 manuscript.

## 542 **Competing interests**

543 The Authors declare that they have no conflict of interest.

## 544 **Acknowledgments**

545 We want to thank the National Institute of Environmental Health Sciences (NIEHS)  
546 support this study, the research project is “Neurological Effects of Environmental styrene and  
547 BTEX Exposure in a Gulf of Mexico Cohort” (Grant No. R01ES031127). We appreciate other  
548 grant support by NOAA Climate Program Office’s Atmospheric Chemistry, Carbon Cycle, and  
549 Climate (AC4) program and Climate Observations and Monitoring (COM) program, Grant No.  
550 NA21OAR4310225 (GMU) / NA21OAR310226 (UMD), and the Fine Particle Research Initiative  
551 in East Asia Considering National Differences (FRIEND) project through the National Research  
552 Foundation of Korea (NRF) funded by the Ministry of Science and ICT (2020M3G1A1114621).  
553 This work was also supported by Korea Environment Industry & Technology Institute (KEITI)  
554 through Project for developing an observation-based GHG emissions geospatial information map,  
555 funded by Korea Ministry of Environment (MOE) (RS-2023-00232066). We also thank the Texas  
556 Commission on Environmental Quality (TCEQ), South Coast Air Quality Management District  
557 (AQMD), Ramboll CAMx team, and the University of North Carolina at Chapel Hill (UNC-CH)  
558 for their invaluable assistance.

559

560

## 561 Reference

- 562 Al-Harbi, M., Alhajri, I., AlAwadhi, A., and Whalen, J. K.: Health symptoms associated with  
563 occupational exposure of gasoline station workers to BTEX compounds, Atmospheric  
564 Environment, 241, 117847, 2020.
- 565 Anaconda: Anaconda python: <https://www.anaconda.com/products/individual>, last access: May,  
566 1st, 2020.
- 567 ATSDR: Toxicological Profile for benzene, <https://www.atsdr.cdc.gov/toxprofiles/tp3.pdf>,  
568 2007a.
- 569 ATSDR: Toxicological Profile for xylene, <https://www.atsdr.cdc.gov/toxprofiles/tp71.pdf>,  
570 2007b.
- 571 ATSDR: Toxicological Profile for ethylbenzene,  
572 <https://www.atsdr.cdc.gov/toxprofiles/tp110.pdf>, 2010a.
- 573 ATSDR: Toxicological Profile for styrene, <https://www.atsdr.cdc.gov/toxprofiles/tp53.pdf>,  
574 2010b.
- 575 ATSDR: Toxicological Profile for toluene, <https://www.atsdr.cdc.gov/toxprofiles/tp56.pdf>,  
576 2017.
- 577 Baek, B. H. and Seppanen, C.: SMOKE v4.8.1 Public Release (January 29, 2021) (Version  
578 SMOKEv481\_Jan2021): <http://doi.org/10.5281/zenodo.4480334> last 2021.
- 579 Bloss, C., Wagner, V., Jenkin, M. E., Volkamer, R., Bloss, W. J., Lee, J. D., Heard, D. E., Wirtz,  
580 K., Martin-Reviejo, M., Rea, G., Wenger, J. C., and Pilling, M. J.: Development of a detailed  
581 chemical mechanism (MCMv3.1) for the atmospheric oxidation of aromatic hydrocarbons,  
582 Atmos. Chem. Phys., 5, 641-664, 10.5194/acp-5-641-2005, 2005.
- 583 Chen, W.-H., Chen, Z.-B., Yuan, C.-S., Hung, C.-H., and Ning, S.-K.: Investigating the  
584 differences between receptor and dispersion modeling for concentration prediction and health  
585 risk assessment of volatile organic compounds from petrochemical industrial complexes, Journal  
586 of environmental management, 166, 440-449, 2016.
- 587 Choi, K.-C., Lee, J.-J., Bae, C. H., Kim, C.-H., Kim, S., Chang, L.-S., Ban, S.-J., Lee, S.-J., Kim,  
588 J., and Woo, J.-H.: Assessment of transboundary ozone contribution toward South Korea using

589 multiple source–receptor modeling techniques, *Atmospheric Environment*, 92, 118-129,  
590 <https://doi.org/10.1016/j.atmosenv.2014.03.055>, 2014.

591 Christensen, M. S., Vestergaard, J. M., d'Amore, F., Gørløv, J. S., Toft, G., Ramlau-Hansen, C.  
592 H., Stockholm, Z. A., Iversen, I. B., Nissen, M. S., and Kolstad, H. A.: styrene exposure and risk  
593 of lymphohematopoietic malignancies in 73,036 reinforced plastics workers, *Epidemiology*, 29,  
594 342-351, 2018.

595 Couzo, E., Olatosi, A., Jeffries, H. E., and Vizuete, W.: Assessment of a regulatory model's  
596 performance relative to large spatial heterogeneity in observed ozone in Houston, Texas, *Journal*  
597 *of the Air & Waste Management Association*, 62, 696-706, 10.1080/10962247.2012.667050,  
598 2012.

599 Declet-Barreto, J., Goldman, G. T., Desikan, A., Berman, E., Goldman, J., Johnson, C.,  
600 Montenegro, L., and Rosenberg, A. A.: Hazardous air pollutant emissions implications under  
601 2018 guidance on US Clean Air Act requirements for major sources, *Journal of the Air & Waste*  
602 *Management Association*, 70, 481-490, 2020.

603 Doherty, B. T., Kwok, R. K., Curry, M. D., Ekenga, C., Chambers, D., Sandler, D. P., and Engel,  
604 L. S.: Associations between blood BTEXS concentrations and hematologic parameters among  
605 adult residents of the U.S. Gulf States, *Environ Res*, 156, 579-587,  
606 10.1016/j.envres.2017.03.048, 2017.

607 Esri, D., HERE, TomTom, Intermap, increment P Corp., GEBCO, USGS, FAO, NPS, NRCAN,  
608 GeoBase, IGN, Kadaster NL, Ordnance Survey, Esri Japan, METI, Esri China (Hong Kong),  
609 Swisstopo, MapmyIndia, and the GIS User Community: *World Topographic Map*, 2013.

610 Hogrefe, C., Gilliam, R., Mathur, R., Henderson, B., Sarwar, G., Appel, K. W., Pouliot, G.,  
611 Willison, J., Miller<sup>2</sup>, R., Vukovich<sup>1</sup>, J., Eyth, A., Talgo, K., Allen, C., and Foley, K.:  
612 CMAQv5.3.2 ozone simulations over the Northern Hemisphere: model performance and  
613 sensitivity to model configuration  
614 Office of Research and Development, 2021.

615 Hsieh, M.-T., Peng, C.-Y., Chung, W.-Y., Lai, C.-H., Huang, S.-K., and Lee, C.-L.: Simulating  
616 the spatiotemporal distribution of BTEX with an hourly grid-scale model, *Chemosphere*, 246,  
617 125722, 2020a.

618 Hsieh, M. T., Peng, C. Y., Chung, W. Y., Lai, C. H., Huang, S. K., and Lee, C. L.: Simulating  
619 the spatiotemporal distribution of BTEX with an hourly grid-scale model, *Chemosphere*, 246,  
620 10.1016/j.chemosphere.2019.125722, 2020b.



621 Jenkin, M. E., Young, J. C., and Rickard, A. R.: The MCM v3.3.1 degradation scheme for  
622 isoprene, *Atmospheric Chemistry and Physics*, 15, 11433-11459, 10.5194/acp-15-11433-2015,  
623 2015.

624 Lindhjem, C., Chan, L., Pollack, A., Corporation, E. I., Way, R., and Kite, C.: Applying  
625 Humidity and Temperature Corrections to On and Off-Road Mobile Source Emissions, 13th  
626 International Emission Inventory Conference, Clearwater, FL2004.

627 Miller, L., Xu, X. H., Wheeler, A., Zhang, T. C., Hamadani, M., and Ejaz, U.: Evaluation of  
628 missing value methods for predicting ambient BTEX concentrations in two neighbouring cities  
629 in Southwestern Ontario Canada, *Atmospheric Environment*, 181, 126-134,  
630 10.1016/j.atmosenv.2018.02.042, 2018.

631 Moshiran, V. A., Karimi, A., Golbabaee, F., Yarandi, M. S., Sajedian, A. A., and Koozekonan,  
632 A. G.: Quantitative and semiquantitative health risk assessment of occupational exposure to  
633 styrene in a petrochemical industry, *Safety and health at work*, 12, 396-402, 2021.

634 NASA: OZONE & AIR QUALITY: <https://ozoneaq.gsfc.nasa.gov>, last 2021.

635 NCHS: National Center for Health Statistics (NCHS) National Health and Nutrition Examination  
636 Survey Data.: <https://www.cdc.gov/nchs/nhanes/index.htm>, last 2021.

637 Niaz, K., Bahadar, H., Maqbool, F., and Abdollahi, M.: A review of environmental and  
638 occupational exposure to xylene and its health concerns, *EXCLI journal*, 14, 1167, 2015.

639 NIEHS: GuLF STUDY: <https://gulfstudy.nih.gov/en/index.html>, last access: 16, November,  
640 2021.

641 O'Leary, B. F. and Lemke, L. D.: Modeling spatiotemporal variability of intra-urban air  
642 pollutants in Detroit: A pragmatic approach, *Atmospheric Environment*, 94, 417-427,  
643 10.1016/j.atmosenv.2014.05.010, 2014.

644 P.J. Linstrom and W.G. Mallard, E.: NIST Chemistry WebBook, NIST Standard Reference  
645 Database Number 69: <https://webbook.nist.gov/chemistry/>, last 2018.

646 Pankow, J. F., Luo, W. T., Bender, D. A., Isabelle, L. M., Hollingsworth, J. S., Chen, C., Asher,  
647 W. E., and Zogorski, J. S.: Concentrations and co-occurrence correlations of 88 volatile organic  
648 compounds (VOCs) in the ambient air of 13 semi-rural to urban locations in the United States,  
649 *Atmospheric Environment*, 37, 5023-5046, 10.1016/j.atmosenv.2003.08.006, 2003.

650 Polvara, E., Roveda, L., Invernizzi, M., Capelli, L., and Sironi, S.: Estimation of Emission  
651 Factors for Hazardous Air Pollutants from Petroleum Refineries, *Atmosphere*, 12, 1531, 2021.

652 Rahimpoor, R., Sarvi, F., Rahimnejad, S., and Ebrahimi, S. M.: Occupational exposure to BTEX  
653 and styrene in West Asian countries: a brief review of current state and limits, *Archives of*  
654 *Industrial Hygiene and Toxicology*, 73, 107-118, 2022.

655 Rajabi, H., Mosleh, M. H., Mandal, P., Lea-Langton, A., and Sedighi, M.: Emissions of volatile  
656 organic compounds from crude oil processing—Global emission inventory and environmental  
657 release, *Science of The Total Environment*, 727, 138654, 2020.

658 Ramboll: Speciation Tool User’s Guide:  
659 [https://www.cmascenter.org/speciation\\_tool/documentation/5.0/Ramboll\\_sptool\\_users\\_guide\\_V](https://www.cmascenter.org/speciation_tool/documentation/5.0/Ramboll_sptool_users_guide_V5.pdf)  
660 [5.pdf](https://www.cmascenter.org/speciation_tool/documentation/5.0/Ramboll_sptool_users_guide_V5.pdf), last 2020a.

661 RAMBOLL: CAMx7.00 User’s Guide: [https://camx-](https://camx-wp.azurewebsites.net/Files/CAMxUsersGuide_v7.00.pdf)  
662 [wp.azurewebsites.net/Files/CAMxUsersGuide\\_v7.00.pdf](https://camx-wp.azurewebsites.net/Files/CAMxUsersGuide_v7.00.pdf), last 2020b.

663 RAMBOLL: Comprehensive Air Quality Model with Extensions, CAMx:  
664 <https://www.camx.com>, last access: Nov 29, 2021.

665 SRI: Directory of Chemical Producers: United States of America,  
666 <https://books.google.com/books?id=Nx0vAQAAIAAJ>, 2008.

667 Strum, M., Kosusko, M., Shah, T., and Ramboll: SPECIATE and using the Speciation Tool to  
668 prepare VOC and PM chemical speciation profiles for air quality modeling,  
669 [https://cfpub.epa.gov/si/si\\_public\\_file\\_download.cfm?p\\_download\\_id=532731&Lab=NRMRL](https://cfpub.epa.gov/si/si_public_file_download.cfm?p_download_id=532731&Lab=NRMRL),  
670 2017.

671 TCEQ: 2015 Ozone NAAQS Transport SIP Modeling (2012 Episode):  
672 <https://www.tceq.texas.gov/airquality/airmod/data/gn/gn2012>, last access: Nov 18, 2015.

673 TCEQ: TCEQ 2012 Modeling Platform Technical Support Document, [https://wayback.archive-](https://wayback.archive-it.org/414/20210529054550/https://www.tceq.texas.gov/assets/public/implementation/air/am/mo)  
674 [it.org/414/20210529054550/https://www.tceq.texas.gov/assets/public/implementation/air/am/mo](https://wayback.archive-it.org/414/20210529054550/https://www.tceq.texas.gov/assets/public/implementation/air/am/mo)  
675 [deling/gn/doc/TCEQ\\_2012\\_Modeling\\_Platform\\_TSD.pdf](https://wayback.archive-it.org/414/20210529054550/https://www.tceq.texas.gov/assets/public/implementation/air/am/mo), 2016.

676 The R Foundation: The R Project for Statistical Computing: <https://www.r-project.org>, last  
677 access: Jan, 25th, 2022, 2021.

678 UNC-IE: CMAS data warehouse: <https://dataverse.unc.edu/dataverse/ctmascenter>, last access:  
679 Jan, 25th, 2023, 2021.

680 USEPA: Integrated Risk Information System (IRIS) benzene Integrated Risk Information  
681 System: [https://iris.epa.gov/ChemicalLanding/&substance\\_nmbr=276](https://iris.epa.gov/ChemicalLanding/&substance_nmbr=276), last access: Dec 12, 2000.

682 USEPA: Guidance on the Use of models and other analyses for demonstrating attainment of air  
683 quality goals for ozone, PM2.5 and Regional Haze,  
684 [https://permanent.fdlp.gov/LPS74329/draft\\_final-pm-O3-RH.pdf](https://permanent.fdlp.gov/LPS74329/draft_final-pm-O3-RH.pdf), 2006.

685 USEPA: 2014 Fire NEI Workshop Emissions Processing-SmartFire Details,  
686 [https://www.epa.gov/sites/default/files/2015-09/documents/emissions\\_processing\\_sf2.pdf](https://www.epa.gov/sites/default/files/2015-09/documents/emissions_processing_sf2.pdf), 2015.

687 USEPA: Source Classification Codes (SCCs): [https://sor-scc-  
688 api.epa.gov/sccwebservice/sccsearch/](https://sor-scc-api.epa.gov/sccwebservice/sccsearch/), last access: Dec 5, 2016.

689 USEPA: National Emissions Inventory (NEI) 2011 Version 6 Air Emissions Modeling Platform  
690 (EMP): <https://www.epa.gov/air-emissions-modeling/emissions-modeling-platforms>, last access:  
691 JAN, 27th, 2022, 2021a.

692 USEPA: 2011 Version 6 Air Emissions Modeling Platforms: [https://www.epa.gov/air-emissions-  
693 modeling/2011-version-6-air-emissions-modeling-platforms](https://www.epa.gov/air-emissions-modeling/2011-version-6-air-emissions-modeling-platforms), last access: April, 04, 2022, 2021b.

694 USEPA: Ambient Monitoring Technology Information Center (AMTIC):  
695 <https://www.epa.gov/amtic>, last access: Nov, 18, 2021, 2021c.

696 USEPA: Toxics Release Inventory (TRI) program: [https://www.epa.gov/toxics-release-  
697 inventory-tri-program](https://www.epa.gov/toxics-release-inventory-tri-program), last access: Nov 16, 2021d.

698 USEPA: User's Guide for the AMS/EPA Regulatory Model (AERMOD):  
699 [https://gaftp.epa.gov/Air/aqmg/SCRAM/models/preferred/aermod/aermod\\_userguide.pdf](https://gaftp.epa.gov/Air/aqmg/SCRAM/models/preferred/aermod/aermod_userguide.pdf), last  
700 access: August 15, 2023, 2022.

701 USEPA: Air Quality Dispersion Modeling: [https://www.epa.gov/scram/air-quality-dispersion-  
702 modeling#:~:text=Dispersion%20modeling%20uses%20mathematical%20formulations,at%20se  
703 lected%20downwind%20receptor%20locations](https://www.epa.gov/scram/air-quality-dispersion-modeling#:~:text=Dispersion%20modeling%20uses%20mathematical%20formulations,at%20selected%20downwind%20receptor%20locations)., last access: August 15, 2023, 2023.

704 Wang, C.-T. and Baek, B. H.: Hazardous Air Pollutants Imputation (HAPI) (v1.0.1):  
705 <https://doi.org/10.5281/zenodo.7987106>, last access: May 30, 2023, 2023.

706 Wang, C.-T., Baek, B. H., Vizuete, W., and Engel, L. S.: The styrene, benzene, toluene,  
707 ethylbenzene and xylenes (SBTEX) hourly gridding modeled emission and concentration in the  
708 U.S. Gulf region (1), Zenodo [dataset], 10.5281/zenodo.7967541, 2023.

709 Werder, E. J., Engel, L. S., Blair, A., Kwok, R. K., McGrath, J. A., and Sandler, D. P.: Blood  
710 BTEX levels and neurologic symptoms in Gulf states residents, *Environmental research*, 175,  
711 100-107, 2019.

712 Werder, E. J., Engel, L. S., Richardson, D. B., Emch, M. E., Gerr, F. E., Kwok, R. K., and  
713 Sandler, D. P.: Environmental styrene exposure and neurologic symptoms in US Gulf coast  
714 residents, *Environment international*, 121, 480-490, 2018.

715

716

717

718 **Tables**

719

720 **Table 1.** The Annual emission rates (metric tons yr<sup>-1</sup>) of styrene, benzene, toluene, ethylbenzene,  
 721 and xylenes (SBTEX) in 2012 including the increases resulting from this work. The percent  
 722 increase from the 2012 National Emission Inventory is given in parentheses. The bold font  
 723 indicates the emission sector with the maximum SBTEX rates.

724

Emission Sectors	benzene tons yr <sup>-1</sup>	toluene tons yr <sup>-1</sup>	xylenes tons yr <sup>-1</sup>	ethylbenzene tons yr <sup>-1</sup>	styrene tons yr <sup>-1</sup>	Total tons yr <sup>-1</sup>	Sectoral share of total
agriculture fire (agfire)	1,128	745	0	0	0	1,873	0.76%
commercial marine vehicle (cmv)	103	16	24	10	11	164	0.07%
non-point source (nonpt)	3,070	16,932	5,156	1,188	777	27,123	11%
non-road vehicle (nonroad)	4,752	13,506	14,265	2,682	171	35,376	14%
on-road vehicle (onroad)	10,495	<b>43,657</b>	<b>27,271</b>	<b>7,472</b>	309	<b>89,204</b>	36%
wild fire (ptfire)	<b>46,052</b>	10,909	4,355	0	0	61,316	25%
Rail (rail)	10	14	20	8	9	61	0.02%
residential wood combustion (rwc)	395	92	26	0	0	513	0.21%
non-point oil gas industry (np_oilgas)	5,421	2,694 (+69%)	4,683 (+51%)	455 (+100%)	2 (+100%)	13,255 (+28%)	5.4%
electricity power plants unit (ptegu)	277	131 (+2%)	60 (+3%)	35 (+3%)	7 (0%)	510 (+1%)	0.21%
point source emission other than electricity generation unit (ptnonipm)	7,305	2,608 (+17%)	2,644 (+12%)	667 (+12%)	<b>2,911</b> (+34%)	16,135 (+10%)	5.9%
point source emission of oil and gas industry (pt_oilgas)	510	314 (+25%)	209 (+24%)	36 (+24%)	2 (+100%)	1071 (+11%)	0.43%
Total	79,518	90,080 (+2%)	58,713 (+3%)	12,553 (+3%)	4,199 (+22%)	246,601 (+2%)	100%

725

726

727

728 **Table 2.** Normalized Mean Bias (NMB, %) and Correlation Coefficient (R) comparison of average  
 729 observational data and model result during the model simulation period, May 1<sup>st</sup>, 2012 to Sep 30<sup>th</sup>, 2012  
 730 for the 2012 National Emission Inventory (Base), and the emission scenario adjusted in this study (Adj).  
 731 Bold font indicates the model improvement, and gray color font indicates poorer model performance.  
 732 Also shown is the count (N) of available daily average data across all sites.

733

	Group	N	benzene	toluene		xylenes		ethylbenzene		styrene		SBTEX	
				Base	Adj	Base	Adj	Base	Adj	Base	Adj	Base	Adj
<b>R (daily average comparison for all sites)</b>	All	2717	0.54	0.57	0.57	0.58	0.56	0.56	<b>0.56</b>	0.55	<b>0.57</b>	0.65	0.65
<b>R (5 month average comparison for all sites)</b>	All	46	0.68	0.46	0.46	0.79	0.77	0.76	<b>0.77</b>	0.63	<b>0.64</b>	0.75	0.75
<b>NMB (%) (average comparison for all sites)</b>	All	46	12.53	-10.2	<b>-6.7</b>	-30.6	<b>-24.9</b>	-25.2	<b>-21.4</b>	17.4	32.1	-8.8	<b>-5.6</b>
<b>NMB (%) (daily average comparison for all sites)</b>	Rural	508	-22.3	-10.6	<b>-5.4</b>	-33.2	<b>-19.8</b>	-26.8	<b>-23.0</b>	-63.9	<b>-54.8</b>	-19.3	<b>-13.9</b>
	Airport	95	-41.0	-4.5	<b>0.6</b>	-18.4	1.5	-26.0	<b>-19.5</b>	34.5	42.3	-11.8	<b>-5.0</b>
	Urban	272	61.7	82.9	87.5	-20.9	<b>-8.8</b>	17.0	19.9	-50.6	<b>-39.9</b>	32.6	39.3
	Industry	1842	88.0	-6.6	<b>-2.2</b>	-26.5	<b>-23.5</b>	-9.4	<b>-4.9</b>	54.6	76.1	15.5	19.0

734

735

736

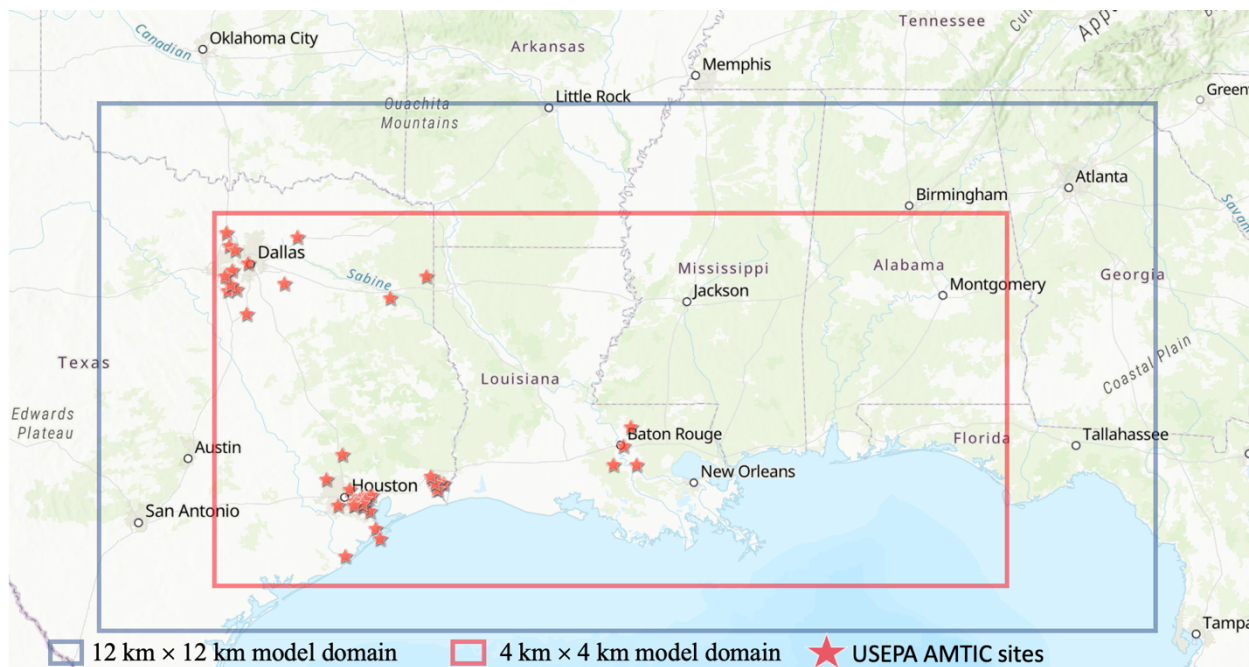
737

738 **Figures:**

739

740

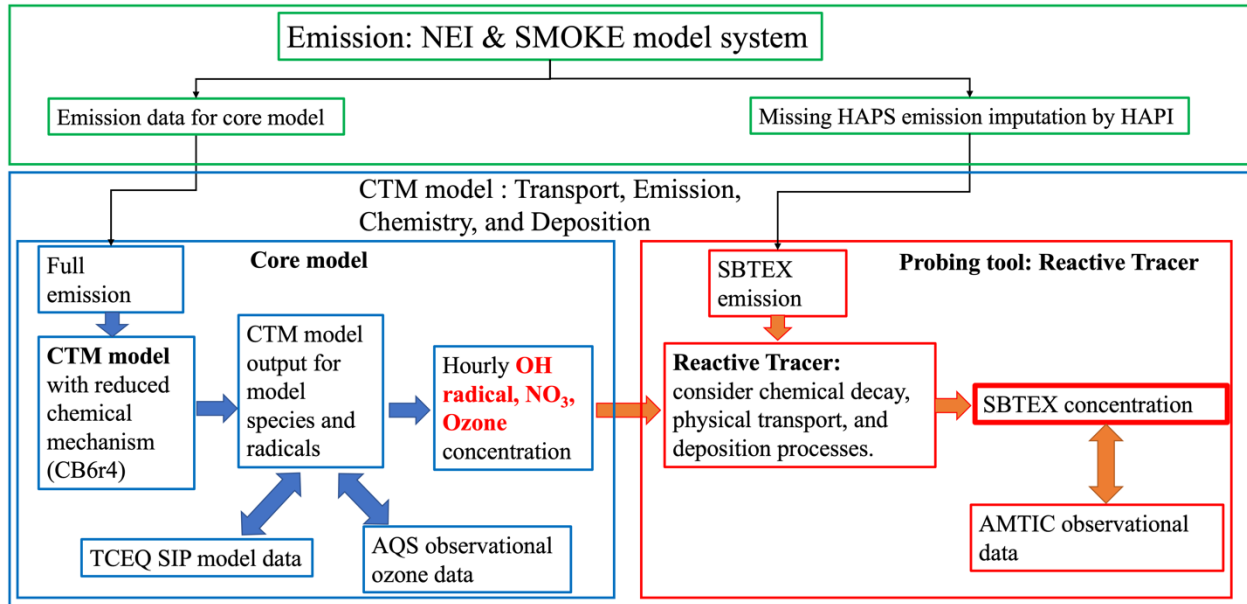
741



742

743 **Figure 1.** The modeling domains with the outer 12 × 12 km resolution domains (blue rectangle)  
744 and inner 4 × 4 km resolution domain (red rectangle). The red stars are the USEPA Ambient  
745 Monitoring Technology Information Center observational (AMTIC) sites for Hazardous Air  
746 Pollutants (HAPs). There are 4 sites are in Louisiana, and 42 sites in Texas. Generated with  
747 ArcGIS map (Esri, 2013).

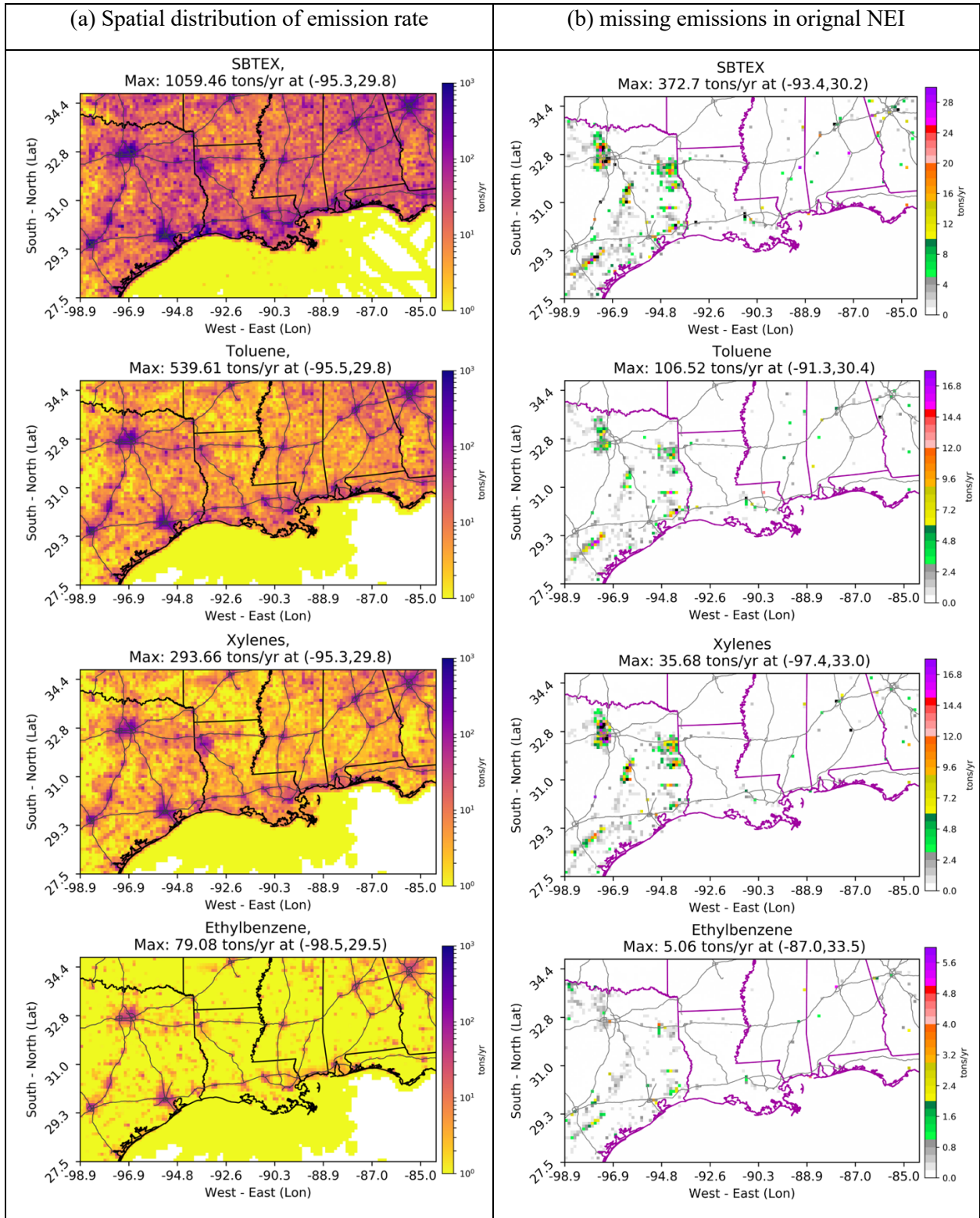
748

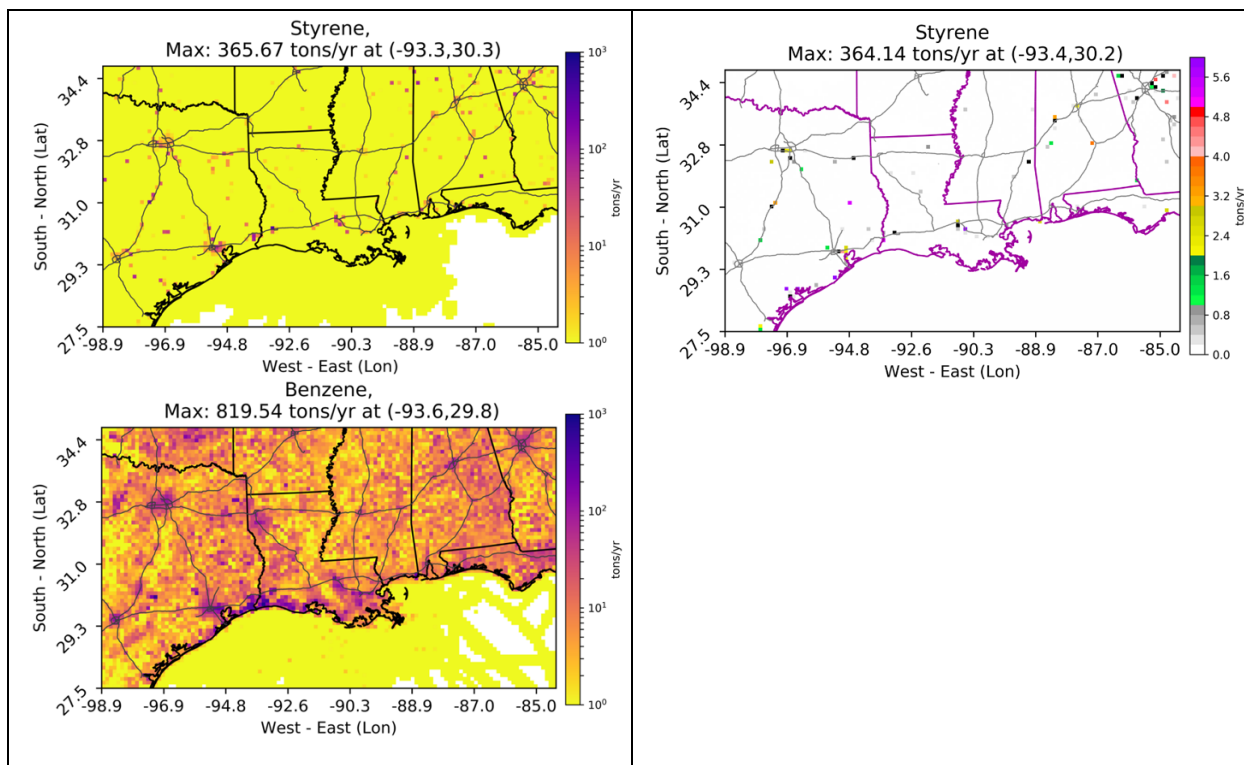


749  
750  
751  
752  
753  
754

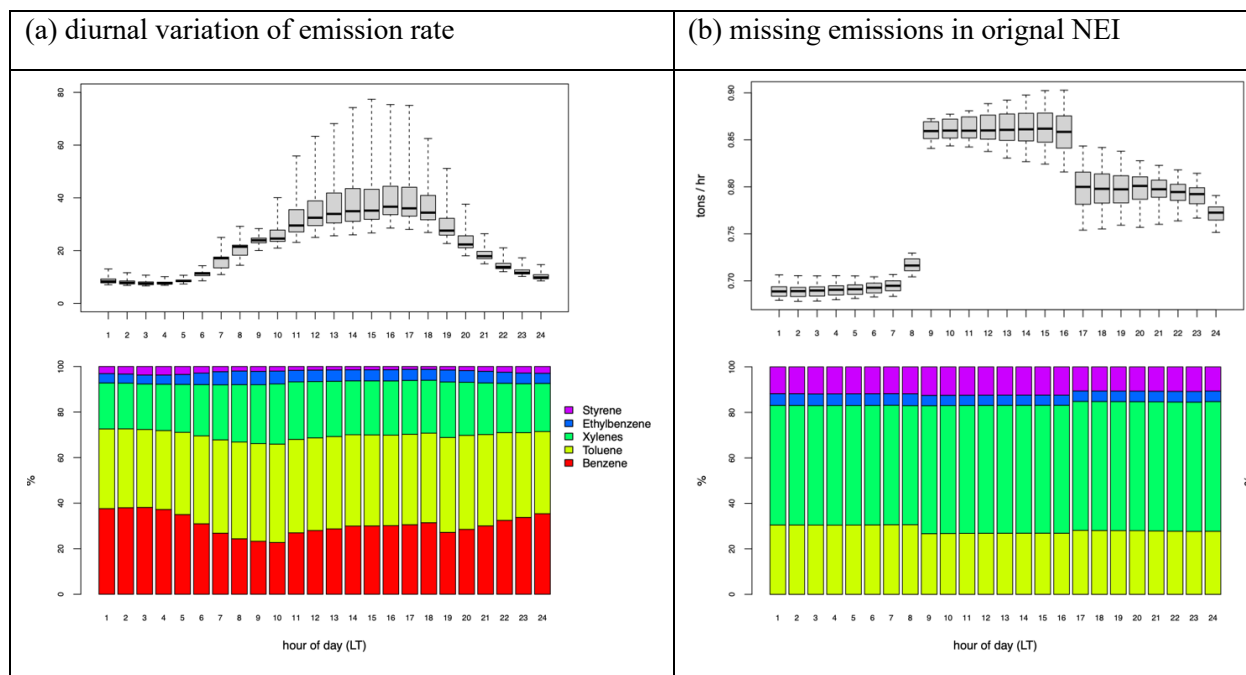
**Figure 2.** Toxic air quality modeling system schematic: The green rectangles are emission processes; the blue rectangles are the base CTM model process for estimating the concentration of oxidants; the red rectangles are the Reactive Tracer process for estimating individual SBTEX concentration.





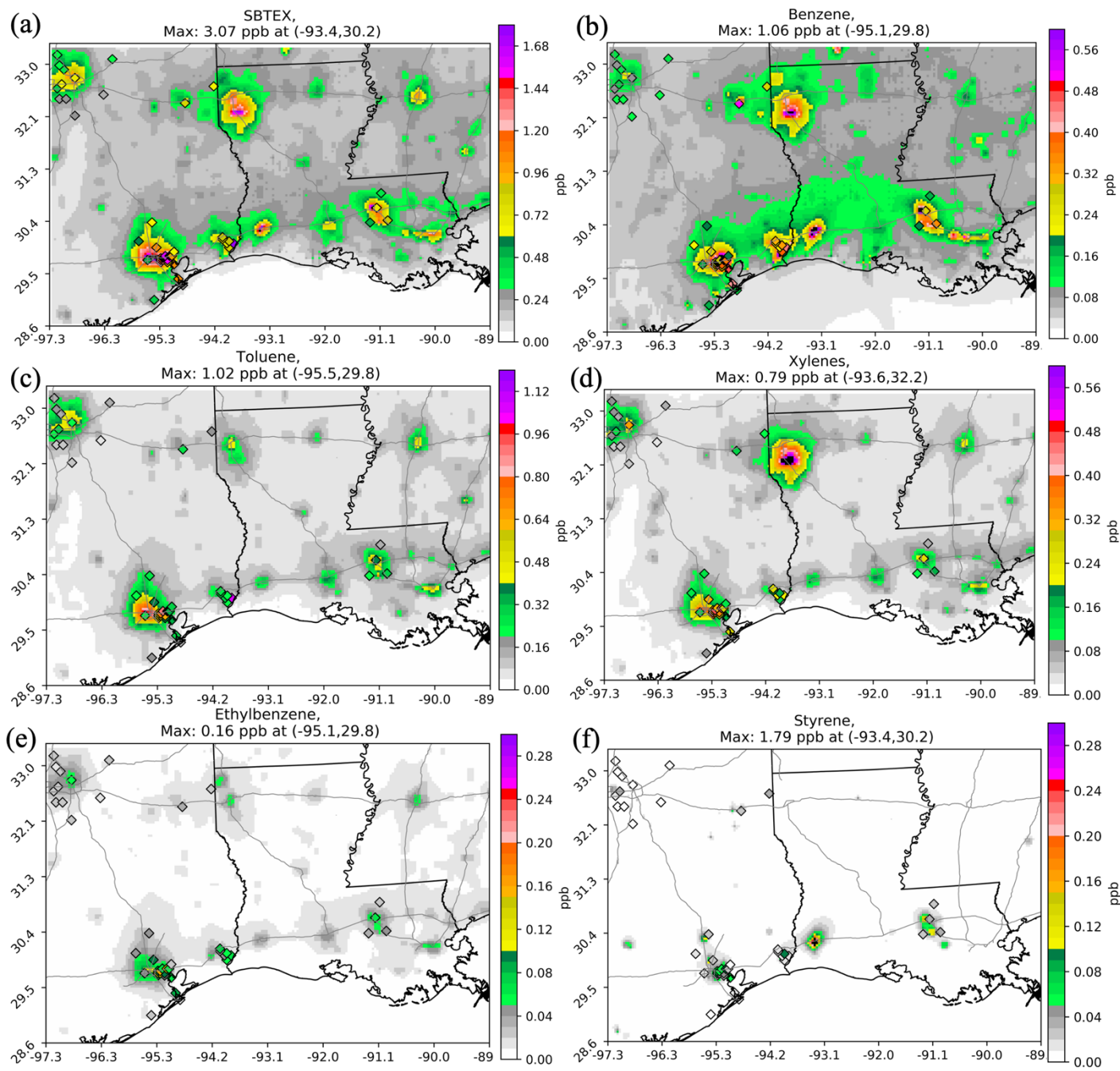


756 **Figure 3.** Spatial distribution of 2012 annual total SBTEX emission rates (ton/yr) of the  
 757 modified emission inventory used in this work (a), and the location and amount of emissions that  
 758 were added to the NEI (b).



760

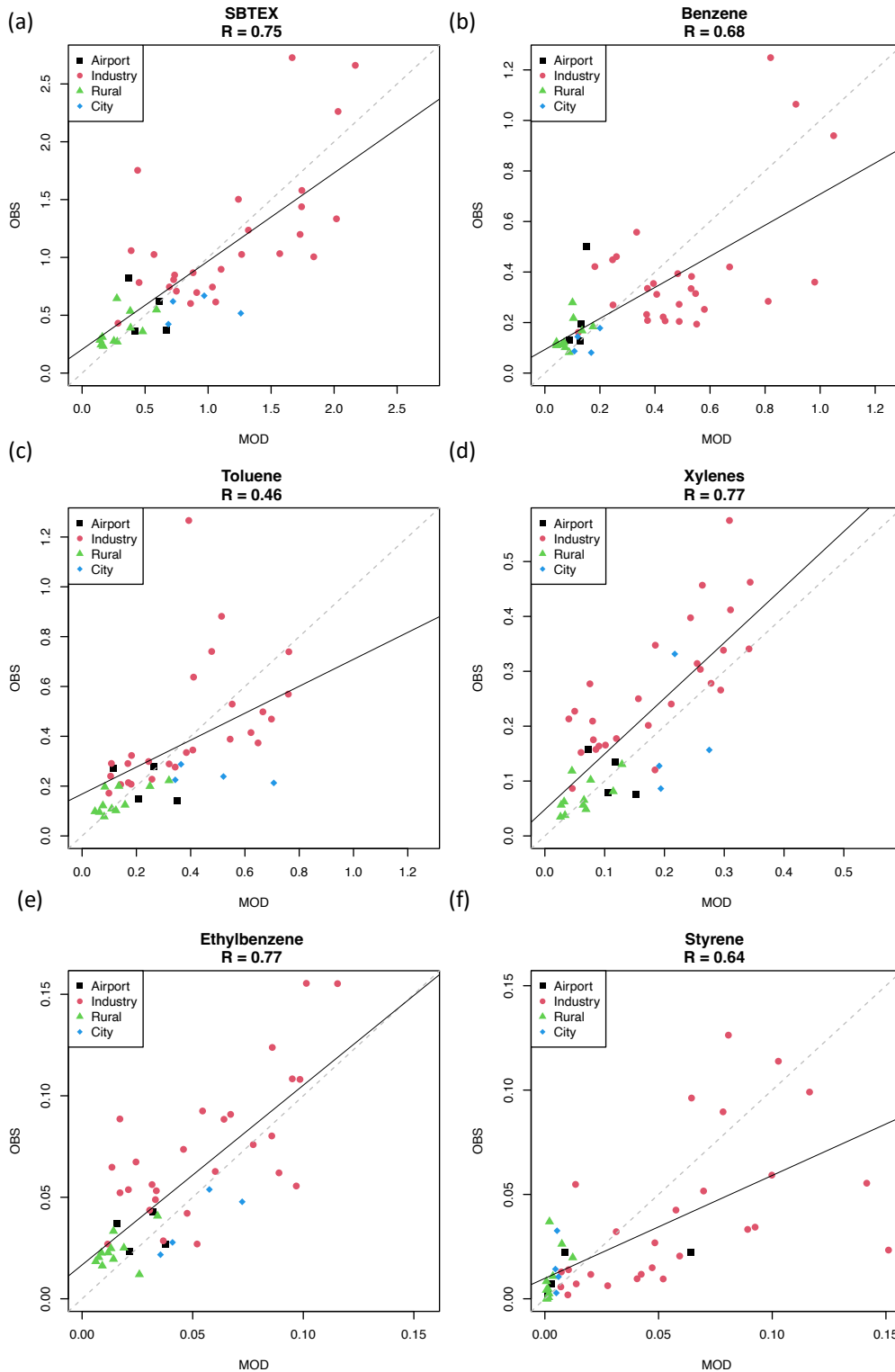
761 **Figure 4.** Diurnal emission pattern of sum styrene, benzene, toluene, ethylbenzene, and xylenes  
 762 (SBTEX) (domain total, tons hr<sup>-1</sup>) (upper panel) and the average relative composition of five  
 763 species (lower panel).



764

765 **Figure 5** (a) The average concentration in Adj scenario overlapped the average observational  
 766 measurement data (Diamond shape) during the model simulation period (May 1<sup>st</sup>, 2012 to Sep  
 767 30<sup>th</sup>, 2012) for (a) Total SBTEX, (b) benzene, (c) toluene, (d) xylenes, (e) ethylbenzene, (f)  
 768 styrene.

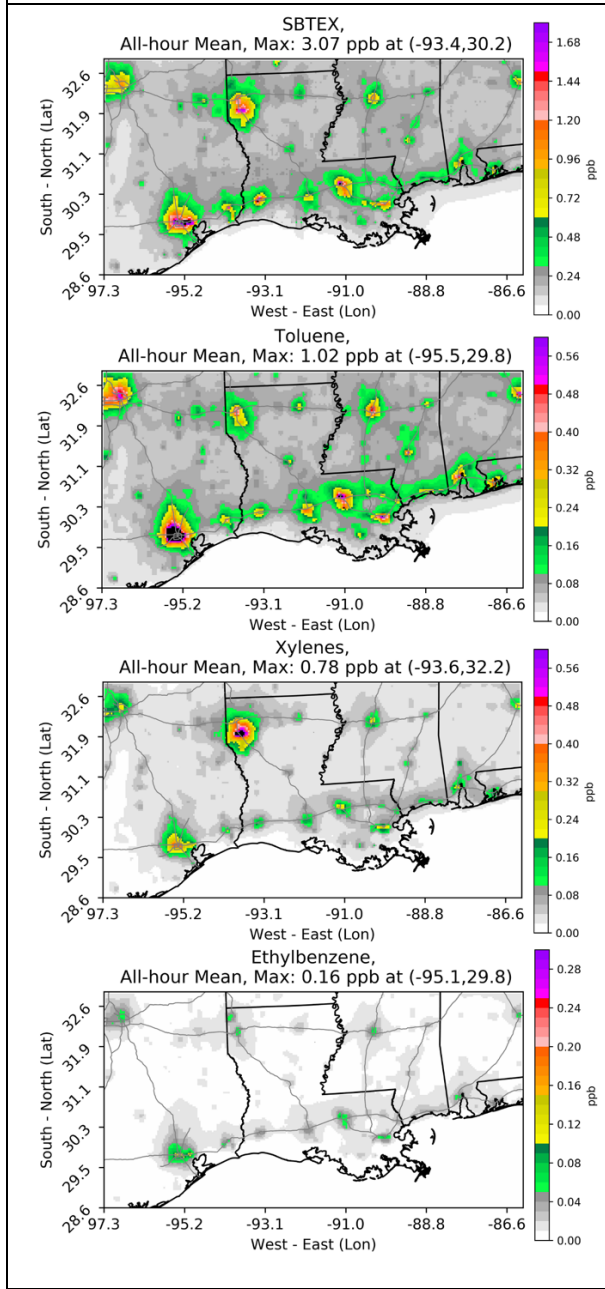
769



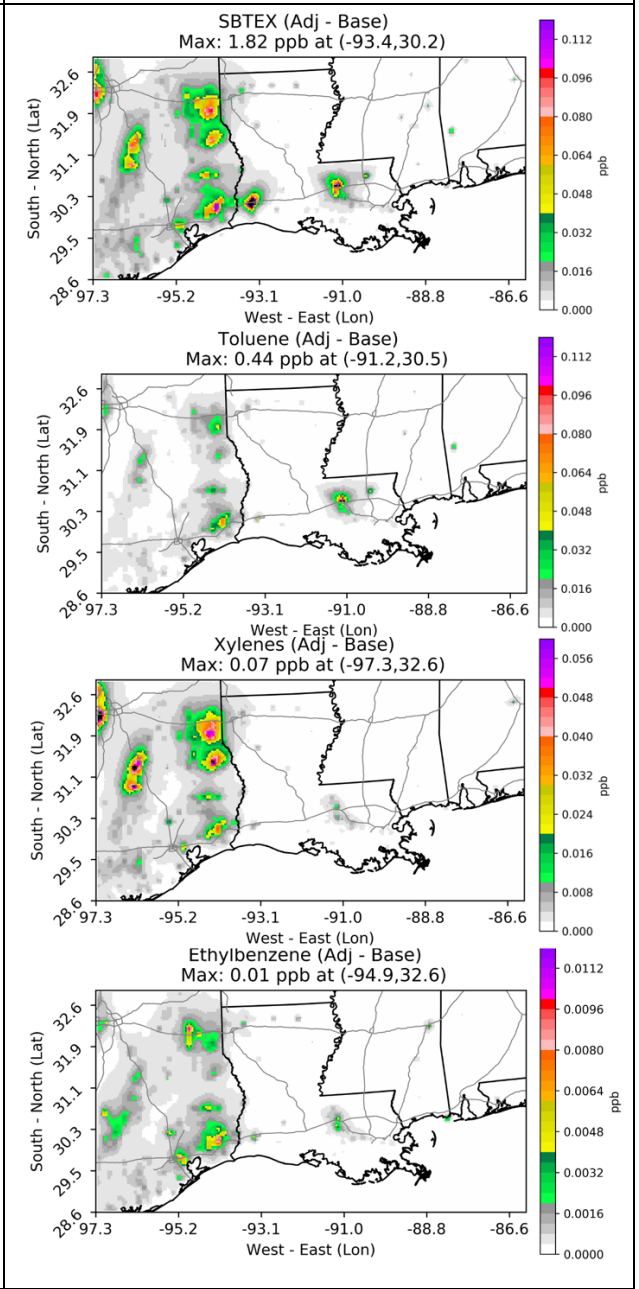
770

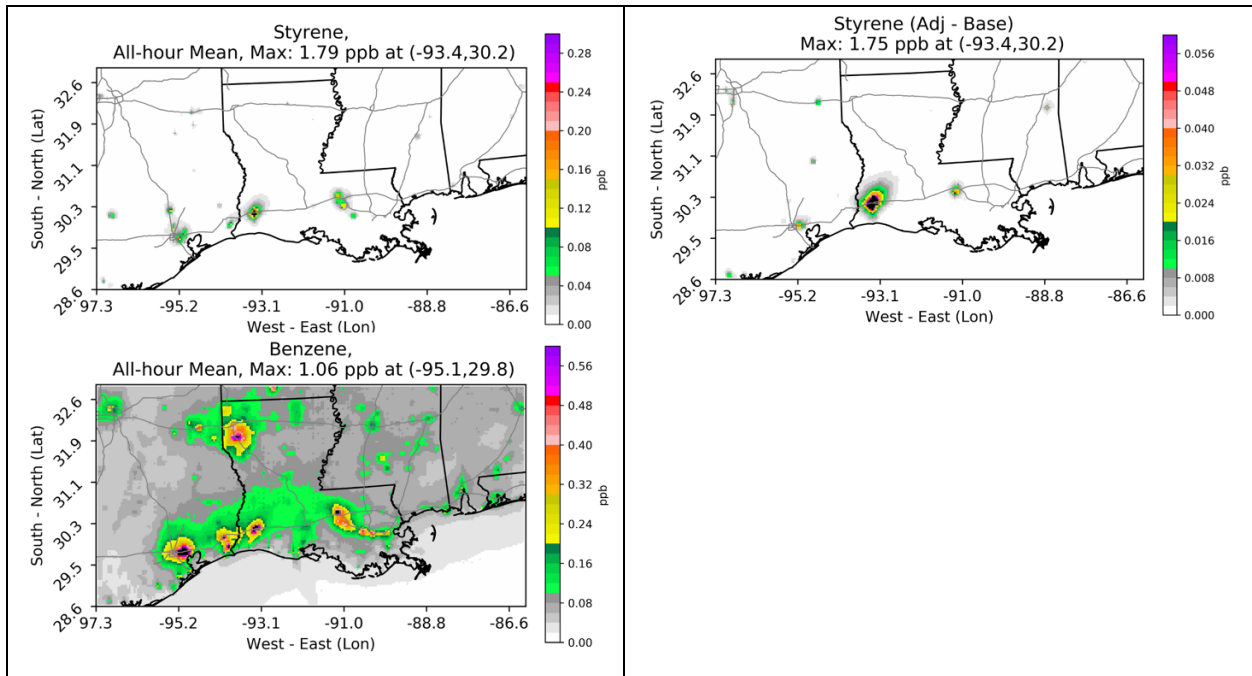
771 **Figure 6.** The average SBTEX concentration (ppb) comparison between model (MOD) Adj case  
 772 and observational (OBS) data during the model simulation period (May 1<sup>st</sup>, 2012 to Sep 30<sup>th</sup>,  
 773 2012) for (a) total SBTEX, (b) benzene, (c) toluene, (d) xylenes, (e) ethylbenzene, and (f) styrene

(a) average concentrations in Adj



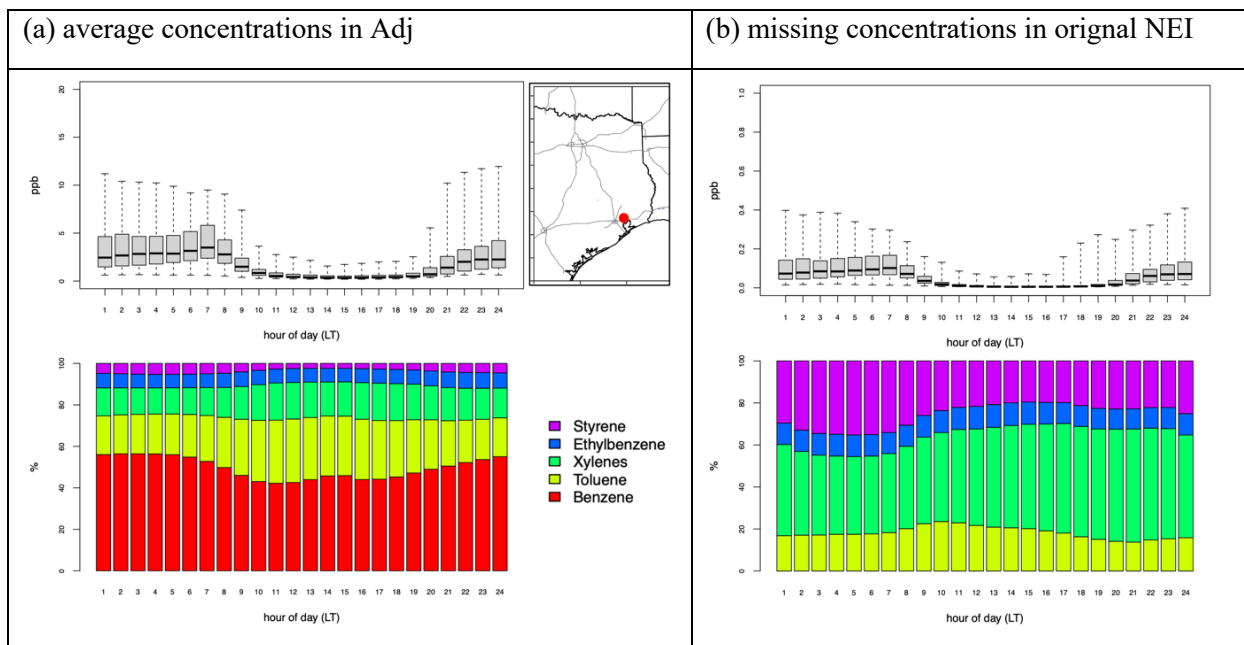
(b) missing concentrations in original NEI





774 **Figure 7.** The average concentration of SBTEX during the model simulation period (May 1<sup>st</sup>,  
 775 2012 to Sep 30<sup>th</sup>, 2012) in Adj scenario. The black color indicates the concentration is higher  
 776 than max color scale bar.

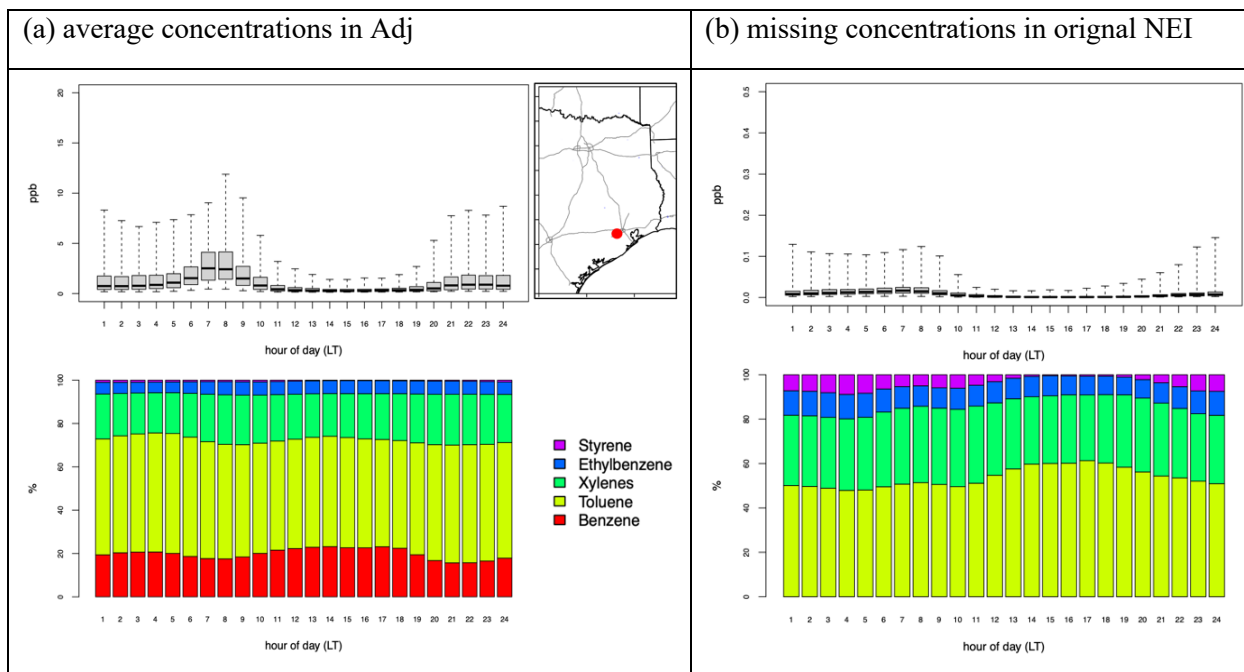
777



778

779 **Figure 8.** Diurnal pattern (upper panel) and relative composition (lower panel) of SBTEX  
 780 concentrations from May 1<sup>st</sup> to September 30<sup>th</sup> in Houston Ship Channel industry area,  
 781 Channelview city (red dot location)





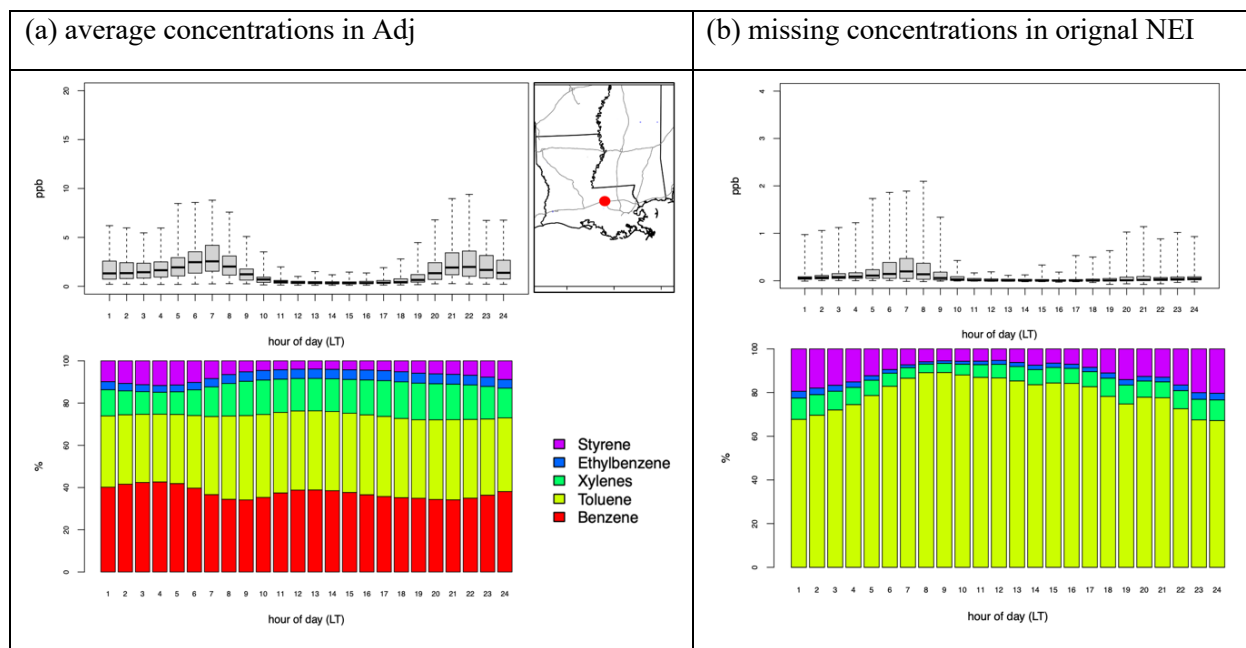
782

783 **Figure 9.** Diurnal pattern (upper panel) and relative composition (lower panel) of SBTEX  
 784 concentrations from May 1<sup>st</sup> to September 30<sup>th</sup> in Houston residential area near Bayland Park  
 785 (red dot location).

786

787

788



789

790 **Figure 10.** Diurnal pattern (upper panel) and relative composition (lower panel) of SBTEX  
791 concentrations from May 1<sup>st</sup> to September 30<sup>th</sup> in Baton Rouge city (red dot location).

792

793